EMERGENCE OF LARGE-SCALE MAGNETIC-VORTICES STRUCTURES BY SMALL-SCALE HELICITY IN STRATIFIED MAGNETIZED PLASMA

Michael I. Kopp[1*], **Volodymyr V. Yanovsky**[1,2]

[1]*Institute for Single Crystals, NAS Ukraine, Nauky Ave. 60, Kharkiv, 61072, Ukraine*
[2]*V.N. Karazin Kharkiv National University, 4, Svoboda Sq., Kharkiv, 61022, Ukraine*
Corresponding Author e-mail: michaelkopp0165@gmail.com

In this paper, a new type of instability is identified, leading to the generation of vortex motions and magnetic fields in a plasma layer with a constant temperature gradient, subjected to uniform gravity and a vertical magnetic field. The analysis in this study is conducted within the framework of electron magnetohydrodynamics (EMHD), taking into account thermomagnetic effects. A new large-scale instability of the α-effect type is identified, which facilitates the generation of large-scale vortex and magnetic fields. This instability arises due to the combined action of an external uniform magnetic field, oriented perpendicular to the plasma layer, and a small-scale helical force. The external force is modeled as a source of small-scale oscillations in the electron velocity field, characterized by a low Reynolds number ($R \ll 1$). The presence of a small parameter in the system allows for the application of the method of multiscale asymptotic expansions, leading to the derivation of nonlinear equations governing the evolution of large-scale vortex and magnetic perturbations. These equations are obtained at third order in the Reynolds number. A new effect associated with the influence of thermal forces (the Nernst effect) on large-scale instability is also discussed. It is shown that an increase in the Nernst parameter reduces the α-coefficient and thereby suppresses the development of the large-scale instability. Using numerical analysis, stationary solutions of the vortex and magnetic dynamo equations are obtained in the form of localized helical-type structures.

Keywords: *electron magnetohydrodynamics, multiscale asymptotic expansions, small-scale force, α-effect, localized structures*

PACS: 47.32.C, 47.35.Fg, 52.25.Xz

1. INTRODUCTION

The investigation of magneto-vortex structures in plasma is of significant importance for addressing challenges in controlled thermonuclear fusion as well as for understanding the formation of ordered structures in astrophysical plasmas. Magneto-vortex structures represent spatially localized configurations in which magnetic fields are strongly coupled with vortical plasma flows (velocity vortices). Such structures frequently emerge in turbulent plasma environments, where instabilities and nonlinear interactions between electric currents, magnetic fields, and hydrodynamic perturbations play a crucial role. A notable example of these interactions is the generation of magnetic fields by small-scale turbulent plasma motions with non-zero helicity $\overline{\mathbf{v}^T \mathrm{rot} \mathbf{v}^T} \neq 0$ – this process constitutes a dynamo mechanism that is fundamental to explaining the origin of magnetic fields in astrophysical objects such as planets, stars, and galaxies [1]-[6]. Helical turbulence, in this context, typically refers to turbulent states with broken parity symmetry [4]. From a physical standpoint, helical turbulence arises in systems where mirror symmetry is broken, which can occur due to various factors – most notably, the presence of external fields with pseudovector characteristics, such as magnetic fields (Lorentz force) or the Coriolis force.

Despite considerable progress in the theory of magnetic dynamos [5]-[6], several important issues remain insufficiently addressed. One such problem is the lack of a clear connection between the generation of seed magnetic fields and the turbulent dynamo process, since both problems are considered separately. A potential mechanism for the spontaneous generation of seed magnetic fields in plasmas with non-uniform temperature distributions is the Nernst effect [7]. This phenomenon is associated with the formation of a vortex-like electric field disturbance, $\mathbf{E}'_N \sim [\mathbf{B}' \times \nabla T_0]$, which is oriented orthogonally to both the background temperature gradient ∇T_0 and the magnetic field perturbation $\mathbf{B}'$. Under non-dissipative conditions, Maxwell's equations can be employed to estimate the resulting magnetic field fluctuations induced by this effect as

$$\frac{\partial \mathbf{B}'}{\partial t} = -c\, \mathrm{rot}\, \mathbf{E}'_N \implies \frac{\partial \mathbf{B}'}{\partial t} \sim \mathrm{rot}[\nabla T_0 \times \mathbf{B}'].$$

Laser-produced plasmas provide a representative example where the Nernst effect plays a significant role. In such systems, intense laser irradiation ionizes and heats the target material, giving rise to a plasma with pronounced temperature gradients. These gradients create favorable conditions for the onset of the Nernst effect. A similar mechanism of magnetic field generation is also expected to operate in astrophysical environments, particularly in the outer layers of hot, massive stars, where strong temperature inhomogeneities are present [8].

Ref. [9] investigates the spontaneous generation of magnetic fields driven by Rayleigh-Benard convection in a thin plasma layer subjected to a uniform gravitational field. The seed magnetic fields are generated via a mechanism analogous to the Biermann battery effect [10]. However, unlike the classical Biermann mechanism, magnetic field excitation here occurs when temperature perturbations, T', act along a direction misaligned with the background gravitational stratification $\mathbf{g}$. This misalignment gives rise to an eddy-induced electromotive force (EMF):

$$\mathbf{E}^{(i)} = -\frac{m}{e}\frac{T'}{T_0}\mathbf{g},$$

which contributes to magnetic field generation according to

$$\frac{\partial \mathbf{B}'}{\partial t} \approx \mathrm{rot}\mathbf{E}^{(i)} = \frac{mc}{e}\left[\frac{\nabla T'}{T_0} \times \mathbf{g}\right], \ \Rightarrow \ \ B'_y \cong \frac{mc}{e}\frac{T'}{T_0}\frac{g}{\lambda}t_B,$$

where λ is the characteristic scale of temperature perturbations, t_B is the characteristic time of magnetic fields generation. Then this initial seed magnetic field acts to induce convective motion of charged particles (electrons and ions) in the stratified plasma. Thus the emergence of positive feedback between the magnetic field and temperature perturbations in the evolution equations is a key condition for the onset of thermomagnetic instability and, as a result, the generation of magnetic field. In a complementary study, Ref. [11] explores magnetic field generation in a fully ionized plasma, both in the presence and absence of an external magnetic field. The analysis incorporates the effects of convective heat transport and thermomagnetic phenomena and establishes criteria for the onset of instabilities that facilitate spontaneous magnetic field growth.

Another unresolved issue is the absence of a fully self-consistent nonlinear theory of the magnetic dynamo. As the magnetic field grows in strength, it begins to influence the plasma flows, thereby limiting the applicability of the kinematic dynamo theory. However, the magnetic fields observed in real astrophysical systems typically exist in a nonlinear regime, highlighting the necessity of developing and studying a nonlinear dynamo theory. The nonlinear theory is commonly formulated as an extension of the mean-field dynamo approach, incorporating nonlinear feedback mechanisms. In the review [6], a phenomenological model of the nonlinear dynamo – referred to as "catastrophic quenching" – is discussed. This model is grounded in energy balance arguments and posits that the Lorentz force significantly alters the velocity field only when the magnetic energy becomes comparable to the kinetic energy of the turbulent flow. Accordingly, the model introduces a simplified phenomenological framework that includes a nonlinear dependence of the turbulent transport coefficients:

$$\alpha = \frac{\alpha_0}{1 + B_0^2/\mathcal{B}^2}, \quad \eta_T = \frac{\eta_0}{1 + B_0^2/\mathcal{B}^2},$$

where α_0 and η_0 are the values of the transfer coefficients obtained in the kinematic approximation; η_T – coefficient of turbulent magnetic viscosity, $B_0^2 = \overline{\mathbf{B}} \cdot \overline{\mathbf{B}}$ – mean field energy, $\mathcal{B}^2$ - kinetic energy of the flow. Reference [5] provides an in-depth analysis of numerical simulation results related to geodynamo and solar dynamo processes. It also introduces a magneto-rotational dynamo mechanism, where turbulence arises as a consequence of magnetohydrodynamic (MHD) instabilities. Furthermore, the review addresses emerging challenges in the theory of magnetic field generation in weakly collisional plasmas, highlighting current gaps and directions for future research. Nevertheless, Ref. [5] does not address regimes where high-frequency, small-scale electron oscillations – such as helicon waves – induce magnetic field restructuring in both space and laboratory plasmas. These rapid, localized processes involve only the electron component, evolving against a quasi-static background of ions. The monograph [3] describes several examples of magnetic field generation driven by Langmuir and ion-acoustic plasma oscillations. In turn, Ref. [12] explores the generation of mean magnetic fields by small-scale turbulence within the framework of electron magnetohydrodynamics (EMHD) with a two and one-half dimensional ($2\frac{1}{2}$D) model. In this approach, while the magnetic field retains all three spatial components, its variation is constrained to two dimensions due to the presence of a strong background field. It is demonstrated that the emergence of large-scale magnetic fields is intimately connected to the statistical properties of turbulence: the breaking of reflectional symmetry gives rise to the α-effect, whereas turbulence anisotropy facilitates mechanisms akin to negative dissipation, including negative resistivity and viscosity.

One of the drawbacks of magnetic dynamo theory is that it depends on a simplified approach called the two-scale approximation of mean-field theory, making it harder to create a consistent nonlinear dynamo theory. An alternative approach, based on multiscale asymptotic expansions, was proposed in [13] to describe the generation of large-scale vortex structures (LSVSs) in non-mirror-symmetric turbulence. It was shown that small-scale parity violation due to external forcing leads to a large-scale instability known as the anisotropic kinetic alpha (AKA) effect. Further studies [14] explored the reverse energy cascade and nonlinear saturation of this instability. The effect is interpreted as a parametric instability arising from external periodic forcing $\mathbf{F}_0$, which induces small-scale velocity fluctuations $\mathbf{v}_0$. Their nonlinear interaction with large-scale flow $\mathbf{W}$ modifies the Reynolds stresses, allowing δT_{ij} to be expressed as a Taylor series in gradients of $\mathbf{W}$ [15]:

$$\delta T_{ij} = -\alpha_{ijl}W_l - \nu_{ijlm}\nabla_l W_m + O(\nabla^2 \mathbf{W}) + \dots$$

This expansion is valid under the condition of weak large-scale gradients, i.e., for small $\nabla \mathbf{W}$. To ensure the dominance of the first term in the series, one can estimate the tensors α_{ijl} and ν_{ijlm} using characteristic parameters of the small-scale

turbulence. This yields the condition that the gradient scale of the large-scale field, defined as $L_g = (W^{-1}|\nabla W|)^{-1}$, must be much larger than the turbulence scale l_0: $L_g \gg l_0$. The leading term in this expansion corresponds to the anisotropic kinetic α-effect (AKA-effect), as described in [13], which accounts for the emergence of large-scale vortex structures (LSVS). Thus, an external force breaking parity at small scales can induce significant modifications in the large-scale flow. In contrast, Ref. [15] analyzed the case where the small-scale forcing is parity-invariant, leading to the suppression of the AKA-effect. In this regime, the interaction between small- and large-scale motions is governed primarily by eddy viscosity.

Using the method of multiscale asymptotic expansions, nonlinear theories of vortex dynamos have been developed for a range of hydrodynamic media, as outlined in Ref. [16]. In particular, Ref. [17] identified a large-scale instability in an electrically conducting, temperature-stratified medium driven by the helicity of small-scale velocity and magnetic fields. This instability gives rise to the simultaneous generation of large-scale vortex and magnetic fields. Building upon these results, Ref. [18] formulated a fully nonlinear, self-consistent theory of the magneto-vortex dynamo for a convective, electrically conducting medium with helical small-scale turbulence. Remarkably, this study demonstrated for the first time the possibility of stationary chaotic large-scale structures forming in both vortex and magnetic fields. The analysis revealed the emergence of stationary magnetic structures, which can be categorized into three distinct types: nonlinear waves, solitons, and kink-type solutions. Furthermore, qualitative estimates of the linear instability stage allowed for a comparison of the characteristic scales and times of the resulting hydrodynamic structures with those observed under solar conditions, as reported in Ref. [19], showing good agreement.

In this work, unlike [20], we investigate the generation of large-scale vortex and magnetic structures driven by small-scale helical forcing (turbulence) in a fully ionized, temperature-stratified plasma subjected to an external vertical magnetic field. The theoretical framework is based on the Braginskii equations for the electron component, with thermo-magnetic effects explicitly taken into account. Plasma thermal convection is modeled using the Boussinesq approximation, incorporating an external helical force $\mathbf{F}_0$. Unlike the classical anisotropic kinetic α-effect (AKA-effect), our analysis reveals a novel plasma α-effect arising in a magnetized plasma with a constant temperature gradient and gravitational field, induced by external helical forcing.

The structure of this paper is as follows. In Section 2, we formulate the problem and derive the governing equations in dimensionless form. Section 3 presents the derivation of the averaged equations for large-scale velocity and magnetic fields in a magnetized, stratified plasma using the method of multiscale asymptotic expansions. The detailed procedure for constructing the asymptotic expansion is provided in Appendix A. The correlation functions appearing in the averaged equations are expressed through the small-scale fields obtained in the zeroth-order approximation with respect to the Reynolds number R. The corresponding solutions for the small-scale fields are given in Appendix B. Based on these, the closed-form nonlinear equations describing the vortex and magnetic dynamo are derived in Appendix C. In Section 4, we present the final system of equations governing large-scale velocity and magnetic field perturbations, which describe the hydrodynamic α-effect instability. The conditions for the onset of this instability are analyzed as functions of the external magnetic field strength D, the Rayleigh number Ra, and the Nernst effect parameter. Section 5 provides a numerical investigation of the steady-state nonlinear magneto-vortex dynamo equations, demonstrating the formation of vortex and magnetic structures in the form of helical kink-type solutions.

2. PROBLEM STATEMENT AND BASIC EQUATIONS

We consider a fully ionized plasma layer placed in constant gravitational and uniform magnetic fields, denoted by $\mathbf{g}$ and $\overline{\mathbf{B}}$, respectively. The plasma is assumed to possess a steady-state temperature gradient $\nabla \overline{T}$. In the undisturbed state, no fluid motion is present. The development of perturbations is assumed to occur on timescales short enough that ions can be regarded as stationary and thermally inactive. The behavior of the perturbed electron component is analyzed within the framework of the Braginskii equations [21]:

$$\frac{\partial \mathbf{V}}{\partial t} + (\mathbf{V}\nabla)\mathbf{V} = -\frac{e}{m}\left(\mathbf{E} + \frac{1}{c}[\mathbf{V} \times \mathbf{B}]\right) - \frac{1}{m\overline{N}}\nabla P + \frac{1}{m\overline{N}}(\mathbf{R}_v + \mathbf{R}_T) + \frac{\mathbf{F}_\eta}{m\overline{N}} + \frac{\mathbf{F}_g}{m\overline{N}}, \tag{1}$$

$$\frac{\partial T}{\partial t} + (\mathbf{V}\nabla)T = -\frac{2}{3}\frac{\text{div}\mathbf{q}}{\overline{N}}, \quad P = \overline{N}T, \tag{2}$$

$$\text{div}\mathbf{V} = 0. \tag{3}$$

Here $P, \overline{N}, T, \mathbf{V}$ denote the pressure, average density, temperature, and velocities of electrons. In the electron momentum equation (1), several physical effects are taken into account: electron collisions, described by the friction force $\mathbf{R}_v$; momentum exchange due to the temperature gradient, represented by the thermal force $\mathbf{R}_T$; viscous effects in the electron fluid, captured by the force $\mathbf{F}_\eta$; and the gravitational contribution $\mathbf{F}_g$. Importantly, the corresponding transport coefficients in the presence of a magnetic field depend on the magnetization parameter $\omega_{Be}\tau$, where $\omega_{Be} = eB/mc$ is the electron gyrofrequency. In the strongly magnetized limit ($\omega_{Be}\tau \gg 1$), the friction and thermal forces, $\mathbf{R}_v$ and $\mathbf{R}_T$, respectively, are expressed in specific forms:

$$\frac{\mathbf{R}_v}{m\overline{N}} = -0.51\nu\mathbf{V}_\parallel - \nu\mathbf{V}_\perp \tag{4}$$
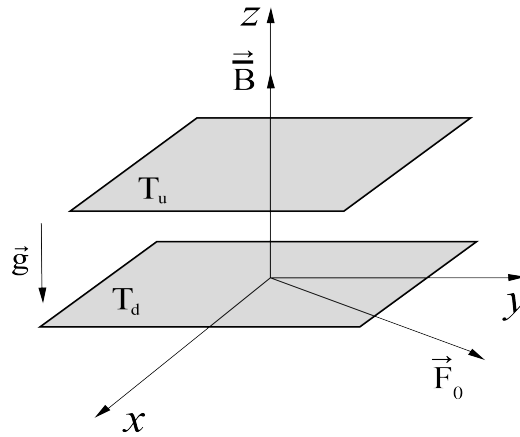
Figure 1. The diagram shows a thin layer of plasma with a vertical equilibrium temperature gradient: $T_d > T_u$ (signaling heating from below). The induction vector $\overrightarrow{\mathbf{B}}$ of a uniform magnetic field has direction along the z-axis, and the external force $\mathbf{F}_0$ is situated in the plane (x, y).

$$\frac{\mathbf{R}_T}{m\overline{N}} = -0.71\frac{\nabla_\| T}{m} - \frac{3}{2}\frac{e\nu}{m^2 c\omega_{Be}^2}[\mathbf{B} \times \nabla T] \tag{5}$$

The symbols $\|$ and $\perp$ denote the directional orientation along and across the magnetic field, respectively. The thermal electron flow is similarly composed of two components, denoted as $\mathbf{q} = \mathbf{q}_\nu + \mathbf{q}_T$:

$$\mathbf{q}_\nu = 0.71\overline{N}T\mathbf{V}_\| + \frac{3e}{2mc}\frac{\nu\overline{N}T}{\omega_{Be}^2}[\mathbf{B} \times \mathbf{V}] \tag{6}$$

$$\mathbf{q}_T = -3.16\frac{\overline{N}T\tau}{m}\nabla_\| T - 4.66\frac{\overline{N}T\nu}{m\omega_{Be}^2}\nabla_\perp T - \frac{5}{2}\frac{e\overline{N}T}{cm^2\omega_{Be}^2}[\mathbf{B} \times \nabla T] \tag{7}$$

In expressions (4)-(7), the parameter $\nu \approx \tau^{-1}$ denotes the electron collision frequency. In a fully ionized plasma, the relative velocities involved in electron-electron and electron-ion collisions are of the same order. As a result, the frequency of electron-electron collisions ($\nu_{ee} \approx \tau_e^{-1}$ or $\nu \approx \tau^{-1}$) is comparable to the electron-ion collision frequency ($\nu_{ei} \approx \tau_{ei}^{-1}$).

Next, we supplement the equations (1)-(3) with Faraday's law

$$\text{rot}\mathbf{E} = -\frac{1}{c}\frac{\partial \mathbf{B}}{\partial t}, \tag{8}$$

Ampere's law

$$\text{rot}\mathbf{B} = -\frac{4\pi e\overline{N}}{c}\mathbf{V}, \tag{9}$$

and magnetic field solenoidality equation

$$\text{div}\mathbf{B} = 0. \tag{10}$$

We now formulate the problem, the geometry of which is illustrated in Fig. 1. To describe the dynamics of the electron fluid, we adopt a Cartesian coordinate system with the Z-axis oriented vertically upward. The system under consideration is a horizontally extended plasma layer of finite thickness h, bounded above and below by free surfaces at $z = h$ and $z = 0$, respectively. The lower boundary at $z = 0$ is maintained at temperature T_d, while the upper boundary at $z = h$ is kept at a lower temperature T_u, such that $T_d > T_u$, implying that the layer is heated from below. The equilibrium temperature distribution $\overline{T}(z)$ is assumed to vary linearly along the vertical direction:

$$\overline{T}(z) = T_d - \frac{(T_d - T_u)}{h}z.$$

Consequently, the equilibrium temperature gradient is constant and directed downward: $\nabla\overline{T} = \text{const} = -\mathbf{e}(d\overline{T}/dz) = -\mathbf{e}A$, where $\mathbf{e}$ is a unit vector along the Z-axis pointing upward, and the gravitational acceleration is given by $\mathbf{g} = -g\mathbf{e}$. Initially, the plasma layer is assumed to be at rest. Convection is triggered by introducing small perturbations to the equilibrium state. All relevant physical quantities appearing in Eqs. (1)-(3) are thus represented as the sum of a stationary background and a small disturbance:

$$\mathbf{V} = \mathbf{V}', \ \mathbf{E} = \mathbf{E}', \ \mathbf{B} = \overline{\mathbf{B}} + \mathbf{B}', \ T = \overline{T} + T', \ P = \overline{P} + P'.$$

The equilibrium electron density is assumed to be uniform throughout the layer, $\overline{N} = $ const, and perturbations in the density, N', are related to temperature perturbations T' via the Boussinesq approximation [22]: $N'/\overline{N} \approx -T'/\overline{T}$. Under this approximation, the gravitational force term in Eq. (1) reduces to a contribution that depends linearly on the temperature perturbation:

$$\frac{\mathbf{F}_g}{m\overline{N}} = \frac{N'}{\overline{N}}\mathbf{g} = -\frac{T'}{\overline{T}}\mathbf{g}. \tag{11}$$

The viscous force $\mathbf{F}_\eta$ in equation (1) can be written as [21]

$$\frac{\eta_e}{m\overline{N}}\nabla^2\mathbf{V}' = 0.73\frac{\overline{T}\tau}{m}\nabla^2\mathbf{V}' = \nu\nabla^2\mathbf{V}',$$

where ν is the coefficient of kinematic viscosity of the electronic fluid. Below in the text, for convenience, we omit the "prime" sign above the perturbed values $\mathbf{V}, T, P, \mathbf{E}$, and $\mathbf{B}$. In the equilibrium (unperturbed) state, the plasma satisfies the condition of hydrostatic balance:

$$\frac{1}{m}\frac{d\overline{T}}{dz} = g - \frac{0.71}{m}\frac{d\overline{T}}{dz},$$

and no background electric field is present, i.e., $\overline{\mathbf{E}} = 0$. The magnetic field is assumed to be uniform and directed vertically upward, perpendicular to the (x, y) plane: $\overline{\mathbf{B}} = \mathbf{e}\overline{B}$. To model turbulent processes in the plasma, we introduce an external force $\mathbf{F}_0$ into Eq. (1). This force acts as a driver of small-scale, high-frequency oscillations in the electron velocity field, denoted by $\widetilde{\mathbf{v}}_0$, and operates in a regime characterized by a low Reynolds number, $R = \widetilde{v}_0 t_0/\lambda_0 \ll 1$. An analogous dimensionless parameter, the Strouhal number $S = u\tau_c/\lambda_c$ – where u is the turbulent velocity, and τ_c and λ_c are characteristic temporal and spatial correlation scales is commonly used in magnetic dynamo theory [2] to justify the second-order correlation approximation. A relevant physical system in which the condition $R \ll 1$ (or equivalently $S \ll 1$) holds is the solar convective zone. Using observational data on small-scale turbulence in solar granules [2], one obtains:

$$\widetilde{v}_0 \approx 3 \cdot 10^2 m/s, \ t_0 \approx 3 \cdot 10^2 s, \ \lambda_0 \approx 10^6 m,$$

yielding an estimate of the Reynolds number $R \approx 10^{-1} \ll 1$. Let us consider an external helical force $\mathbf{F}_0$ with the following properties:
1. The vector field $\mathbf{F}_0$ is solenoidal, i.e., it is divergence-free: $\mathrm{div}\mathbf{F}_0 = 0$.
2. The vector field $\mathbf{F}_0$ possesses vorticity: $\mathrm{rot}\mathbf{F}_0 \neq 0$.
3. The helicity of $\mathbf{F}_0$ is nonzero, indicating a helical property: $\mathbf{F}_0\mathrm{rot}\mathbf{F}_0 \neq 0$.

We define the functional form of the external force as

$$\mathbf{F}_0 = f_0\mathbf{F}_0\left(\frac{x}{\lambda_0}; \frac{t}{t_0}\right),$$

where λ_0 is the characteristic spatial scale, t_0 is the characteristic temporal scale, and f_0 denotes the typical amplitude of the force. The external force $\mathbf{F}_0$ induces small-scale oscillations in the velocity field, denoted by $\widetilde{\mathbf{v}}_0$, which are characterized by

$$\widetilde{\mathbf{v}}_0 = \widetilde{v}_0\widetilde{\mathbf{v}}_0\left(\frac{\mathbf{x}}{\lambda_0}, \frac{t}{t_0}\right),$$

where $\widetilde{v}_0$ is the characteristic velocity. Assuming that the external force $\mathbf{F}_0$ satisfies the properties listed in (4), it can be explicitly prescribed in the following deterministic form:

$$F_0^z = 0, \quad \mathbf{F}_{0\perp} = f_0\left(\mathbf{e}_x\cos\phi_2 + \mathbf{e}_y\cos\phi_1\right), \tag{12}$$

where the phases ϕ_1 and ϕ_2 are defined as

$$\phi_1 = \mathbf{k}_1\mathbf{x} - \omega_0 t, \quad \phi_2 = \mathbf{k}_2\mathbf{x} - \omega_0 t, \ \mathbf{k}_1 = k_0(1, 0, 1), \quad \mathbf{k}_2 = k_0(0, 1, 1).$$

The dynamo mechanism operates through the process of energy transfer from small-scale turbulent motions to large-scale flows. The role of the external small-scale force $\mathbf{F}_0$ incorporated into the electron motion equations is to maintain the necessary level of turbulence as a driving source. This force can be specified statistically by defining its correlator:

$$\overline{F_{0i}F_{0m}} = A\delta_{im} + Br_ir_m + H\epsilon_{imn}r_n.$$

However, the statistical approach is considerably more cumbersome, as it requires specifying the functions A, B, and H, and computing rather complex integrals. When the external force is specified dynamically (as in Eq. 12), averaging over rapid oscillations becomes straightforward, which significantly reduces the computational complexity of the problem.

Let us transform equations (1)-(3) and (9)-(11) into a dimensionless form by introducing the following dimensionless variables

$$\mathbf{x} \to \frac{\mathbf{x}}{\lambda_0}, \quad t \to \frac{t}{t_0}, \quad \mathbf{V} \to \frac{\mathbf{V}}{\widetilde{v}_0}, \quad \mathbf{F}_0 \to \frac{\mathbf{F}_0}{f_0}, \quad \mathbf{B} \to \frac{\mathbf{B}_1}{b_0}, \quad T \to \frac{T_1}{\lambda_0 A}, \quad P \to \frac{P_1}{p_0}. \tag{13}$$

Here, $\widetilde{v}0$, $b0$, and p_0 are the characteristic values of small-scale fluctuations of velocity, magnetic field, and pressure, respectively. When transitioning to the dimensionless form of equations (1)-(3) and (8)-(10), it is helpful to introduce a set of relations that connect the turbulent parameters t_0 and λ_0 of the medium:

$$t_0 = \frac{\lambda_0^2}{\nu}, \quad f_0 = \frac{\widetilde{v}_0 \nu}{\lambda_0^2}, \quad p_0 = m\overline{N}\frac{\widetilde{v}_0 \nu}{\lambda_0}, \quad \frac{f_0 t_0}{\widetilde{v}_0} = \frac{cE_0 t_0}{\lambda_0 b_0} = 1,$$

$$\frac{\lambda_0^2 m}{0.73\overline{T}\tau^2} = 1, \quad \frac{eE_0 t_0}{m\widetilde{v}_0} = \frac{eb_0\lambda_0}{mc\widetilde{v}_0} = \frac{\lambda_0\widetilde{v}_0 m\omega_{pe}^2}{eb_0 c} = R^2, \quad \frac{\lambda_0^2}{r_d^2} = R^4, \tag{14}$$

where $r_d = c/\omega_{pe}$ is the Debye radius, and $\omega_{pe} = \sqrt{4\pi e^2 N_0/m}$ is the electron plasma (Langmuir) frequency. These relations significantly simplify the resulting dimensionless equations, facilitating further mathematical treatment. The first group of relations in (2) is derived from the Navier-Stokes equation (1). The remaining expressions are obtained by applying scaling and dimensional analysis for convenience. The final set of relations is chosen such that a self-consistent system of equations for large-scale perturbations emerges in the leading order of the asymptotic expansion. Upon applying the transformations (13) and (2) to equations (1)-(3), (8)-(10), and introducing a rescaled temperature $T \to T/R$, we arrive at the desired system of dimensionless equations:

$$\frac{\partial \mathbf{V}}{\partial t} + R(\mathbf{V}\nabla)\mathbf{V} = -\nabla P - R^2\mathbf{E} - D[\mathbf{V}\times\mathbf{e}] - R^3[\mathbf{V}\times\mathbf{B}] + \mathbf{e}\widetilde{Ra}T - \mathbf{V} - $$

$$-\widetilde{Ra}\left(\frac{V_{Te}^2}{g\lambda_0}\right)\left(0.71\nabla T + \frac{3}{2}\widetilde{\xi}D[\mathbf{e}\times\nabla T]\right) + \nu\nabla^2\mathbf{V} + \mathbf{F}_0, \tag{15}$$

$$\frac{\partial T}{\partial t} + R(\mathbf{V}\nabla)T - \left(1 + \frac{5}{3}Pr^{-1}\xi R\right)\mathbf{e}\mathbf{V} = 2.1Pr^{-1}\nabla^2 T + \frac{5}{3}Pr^{-1}\xi(\nabla T\,\mathrm{rot}\mathbf{B}), \tag{16}$$

$$\mathrm{div}\mathbf{V} = 0, \quad \mathrm{div}\mathbf{B} = 0, \tag{17}$$

$$\frac{\partial \mathbf{B}}{\partial t} = -\mathrm{rot}\mathbf{E}, \quad \mathrm{rot}\mathbf{B} = -R^2\mathbf{V}. \tag{18}$$

The equations (2)-(16) have the following notation: $\xi = (\omega_{Be}\tau)^{-1}$ represents the reciprocal of the Hall parameter; $\mathbf{D} = D\mathbf{e}$, $D = (e\overline{B}t_0)/mc = (\omega_{Be}\lambda_0^2)/\nu$ is the electron rotation parameter on the scale λ_0; $\widetilde{Ra} = \frac{Ra}{Pr}$, $Ra = \frac{gA\lambda_0^4}{\overline{T}\nu\chi}$ is the Rayleigh number on the scale λ_0; χ is the thermal diffusivity coefficient of electrons; V_{Te} is the thermal velocity of electrons, $Pr = \nu/\chi$ is the Prandtl number; $\widetilde{\xi} = \nu/(\omega_{Be}^2\lambda_0^2\tau)$ is a parameter characterizing the influence of the Nernst effect. As follows, we call $\widetilde{\xi}$ the Nernst parameter.

In this study, we treat the Reynolds number $R = \frac{v_0 t_0}{\lambda_0}$ as a small expansion parameter, assuming $R \ll 1$. The parameters D, $\widetilde{Ra}$, and Pr are considered to be of arbitrary magnitude. The smallness of R justifies the application of the method of multiscale asymptotic expansions, as described in [4, 13]. This technique differs from the traditional mean-field approach in that it allows for a consistent description of how perturbations evolve across various spatial and temporal scales at each order of the expansion. At the zeroth order of R, small-scale rapidly varying velocity fluctuations $\mathbf{v}_0$ arise due to the action of the external force $\mathbf{F}_0$ on a stationary background. The behavior of these fluctuations is shaped by factors such as vertical stratification and the ambient magnetic field. Although the time-averaged values of these fluctuations are zero, nonlinear effects in higher orders can generate contributions that remain finite upon averaging, thereby influencing the dynamics of the system on larger scales.

The following section outlines the procedure for deriving solvability conditions in the framework of multiscale expansions, which ultimately yield the governing equations for large-scale perturbations.

3. EQUATIONS FOR LARGE-SCALE VORTEX AND MAGNETIC FIELDS

To derive the multiscale asymptotic equations, we introduce a set of fast (small-scale) variables $x_0 = (\mathbf{x}_0, t_0)$, alongside slow (large-scale) variables $X = (\mathbf{X}, T)$. For convenience, we denote derivatives with respect to the fast spatial and temporal variables as $\partial_i = \frac{\partial}{\partial x_0^i}$ and $\partial_t = \frac{\partial}{\partial t_0}$, respectively. Correspondingly, the derivatives with respect to the slow (large-scale) spatial and temporal coordinates are written as:

$$\frac{\partial}{\partial X_i} \equiv \nabla_i, \quad \frac{\partial}{\partial T} \equiv \partial_T.$$

The scaling of slow variables relative to the fast ones is chosen as follows:

$$\mathbf{X} = R^2 \mathbf{x}_0, \quad T = R^4 t_0,$$

where $R \ll 1$ is the small expansion parameter introduced earlier. Using these variable transformations, the differential operators in the governing equations (2)–(18) can be rewritten in a form suitable for asymptotic expansion:

$$\frac{\partial}{\partial x_i} \to \partial_i + R^2 \nabla_i, \quad \frac{\partial}{\partial t} \to \partial_t + R^4 \partial_T \tag{19}$$

The physical quantities $\mathbf{V}$, $\mathbf{E}$, $\mathbf{B}$, P, and T are expressed as asymptotic expansions in powers of the small parameter R:

$$\mathbf{V}(\mathbf{x}, t) = \frac{1}{R}\mathbf{W}_{-1}(X) + \mathbf{v}_0 + R\mathbf{v}_1 + R^2\mathbf{v}_2 + R^3\mathbf{v}_3 + \cdots$$

$$\mathbf{E}(\mathbf{x}, t) = \frac{1}{R}\mathbf{E}_{-1}(X) + \mathbf{E}_0 + R\mathbf{E}_1 + R^2\mathbf{E}_2 + R^3\mathbf{E}_3 + \cdots$$

$$\mathbf{B}(\mathbf{x}, t) = \frac{1}{R}\mathbf{B}_{-1}(X) + \mathbf{B}_0 + R\mathbf{B}_1 + R^2\mathbf{B}_2 + R^3\mathbf{B}_3 + \cdots \tag{20}$$

$$T(\mathbf{x}, t) = \frac{1}{R}T_{-1}(X) + T_0(x_0) + RT_1 + R^2T_2 + R^3T_3 + \cdots$$

$$P(\mathbf{x}, t) = \frac{1}{R^3}P_{-3} + \frac{1}{R^2}P_{-2} + \frac{1}{R}P_{-1} + P_0(x_0) + R(P_1 + \overline{P}_1(X)) +$$

$$+ R^2 P_2 + R^3 P_3 + \cdots$$

In the asymptotic expansions (20), the large-scale components depend solely on the slow variables X, whereas the remaining terms involve both the fast variables x_0 and the slow variables X. We now substitute the expansions (19) and (20) into the system of equations (2)–(18), and collect terms up to and including order R^3. The resulting set of equations is rather lengthy and is therefore presented in Appendix A. The main secular equations (solvability conditions), which ensure the consistency of the multiscale asymptotic expansion for the system (2)–(18), are given by:

$$\partial_T W_{-1}^i + \nabla_k \left(\overline{v_0^k v_0^i} \right) = -\nabla_i \overline{P}_1 - \overline{E}_1^i + \nabla_k^2 W_{-1}^i, \tag{21}$$

$$\partial_T T_{-1} - 2.1 Pm^{-1} \nabla^2 T_{-1} = -1.47 \nabla_k \left(\overline{v_0^k T_0} \right), \tag{22}$$

$$\partial_T B_{-1}^i = -\varepsilon_{ijk} \nabla_j \overline{E}_1^k. \tag{23}$$

Equations (21)–(23) are supplemented by the secular equations derived in Appendix A:

$$-\nabla_i P_{-3} - D\varepsilon_{ijk} W_j e_k + e_i \widetilde{Ra} T_{-1} - W_{-1}^i = 0, \tag{24}$$

$$W_{-1}^z = 0, \ \nabla_i W_{-1}^i = 0, \ \nabla_i B_{-1}^i = 0, \ (\nabla \times \mathbf{B}_{-1})_z = 0 \tag{25}$$

$$W_{-1}^k \nabla_k W_{-1}^i = -\nabla_i P_{-1} - E_{-1}^i - \varepsilon_{ijk} W_{-1}^j B_{-1}^k -$$

$$-\widetilde{Ra}_1 \left(0.71 \nabla_i T_{-1} + \frac{3}{2} \widetilde{\xi} D \varepsilon_{ijk} e_j \nabla_k T_{-1} \right), \tag{26}$$

$$W_{-1}^k \nabla_k T_{-1} = 0, \ \varepsilon_{ijk} \nabla_j E_{-1}^k = 0, \ \varepsilon_{ijk} \nabla_j B_{-1}^k = -W_{-1}^i. \tag{27}$$

The primary secular equations that dictate the development of large-scale vortex and magnetic perturbations are represented by Eqs. (21)-(23). In these equations, the overbar signifies averaging over the rapid variables. The extensive temperature T_{-1} does not influence the dynamics of the extensive velocity field $\mathbf{W}_{-1}$ or the magnetic field $\mathbf{B}_{-1}$. Consequently, our analysis will concentrate on equations (21) and (23). In this paper, we focus on large-scale structures characterized by horizontal dimensions L_X, L_Y that are much greater than the vertical dimension L_Z:

$$L_X, L_Y \gg L_Z \gg \lambda_0, \quad \text{or} \quad \varepsilon \cong \left(\frac{L_Z}{L_X}, \frac{L_Z}{L_Y} \right) \ll 1, \quad \frac{\lambda_0}{L_Z} \ll 1, \tag{28}$$

where ε denotes the scale anisotropy parameter. This scaling relationship clearly indicates that derivatives with respect to Z dominate over those with respect to the horizontal coordinates:

$$\nabla_Z \equiv \frac{\partial}{\partial Z} \gg \frac{\partial}{\partial X}, \ \frac{\partial}{\partial Y}.$$

Given that the two equations in (25) imply that the large-scale velocity field is two-dimensional and incompressible, and taking into account the scale relations in (28), we assume that all large-scale perturbations depend solely on the vertical coordinate Z. Thus, the velocity and magnetic fields are represented as

$$\mathbf{W}_{-1} = \left(W^x_{-1}(Z),\, W^y_{-1}(Z),\, 0 \right), \quad \mathbf{B}_{-1} = \left(B^x_{-1}(Z),\, B^y_{-1}(Z),\, 0 \right). \tag{29}$$

Then, taking into account the expressions (29), the equations for the large-scale fields (21)-(23) take the following form:

$$\partial_T W_1 + \nabla_Z \left(\overline{v^z_0 v^x_0} \right) = -\overline{E}^x_1 + \nabla^2_Z W_1, \quad W^x_{-1} \equiv W_1, \tag{30}$$

$$\partial_T W_2 + \nabla_Z \left(\overline{v^z_0 v^y_0} \right) = -\overline{E}^y_1 + \nabla^2_Z W_2, \quad W^y_{-1} \equiv W_2, \tag{31}$$

$$\partial_T B_1 = \nabla_Z \overline{E}^y_1, \quad B^x_{-1} \equiv B_1, \tag{32}$$

$$\partial_T B_2 = -\nabla_Z \overline{E}^x_1, \quad B^y_{-1} \equiv B_2, \tag{33}$$

$$\nabla_Z B_2 = W_1, \quad \nabla_Z B_1 = -W_2. \tag{34}$$

The derivation of the closed form of equations (30)-(31) requires the computation of the Reynolds stress terms $T^{31} = \overline{v^z_0 v^x_0}$ and $T^{32} = \overline{v^z_0 v^y_0}$. This, in turn, involves determining the small-scale velocity field $\mathbf{v}_0$, as outlined in Appendix B. By substituting equations (32)-(34) into equations (30)-(31), the mean electric field $\overline{E}^{x,y}_1$ is eliminated. As a result, equations (30)-(31) are transformed into a system resembling a nonlinear vortex dynamo:

$$\partial_T (\nabla^2_Z W_1 - W_1) + \nabla^3_Z T^{31} = \nabla^4_Z W_1,$$

$$\partial_T (\nabla^2_Z W_2 - W_2) + \nabla^3_Z T^{32} = \nabla^4_Z W_2. \tag{35}$$

According to Ampere's law (34), large-scale perturbations of the magnetic field are driven by large-scale vortical motions of electrons. Consequently, the nonlinear evolution of large-scale magnetic fields is governed by the following set of nonlinear equations:

$$\partial_T (\nabla^2_Z B_1 - B_1) - \nabla^2_Z T^{32} = \nabla^4_Z B_1,$$

$$\partial_T (\nabla^2_Z B_2 - B_2) + \nabla^2_Z T^{31} = \nabla^4_Z B_2. \tag{36}$$

Appendix C presents the calculation of the Reynolds stresses (6), which enables the closure of system (3), and, consequently, (3). The nonlinear magnetic-vortex dynamo is described by the following set of equations:
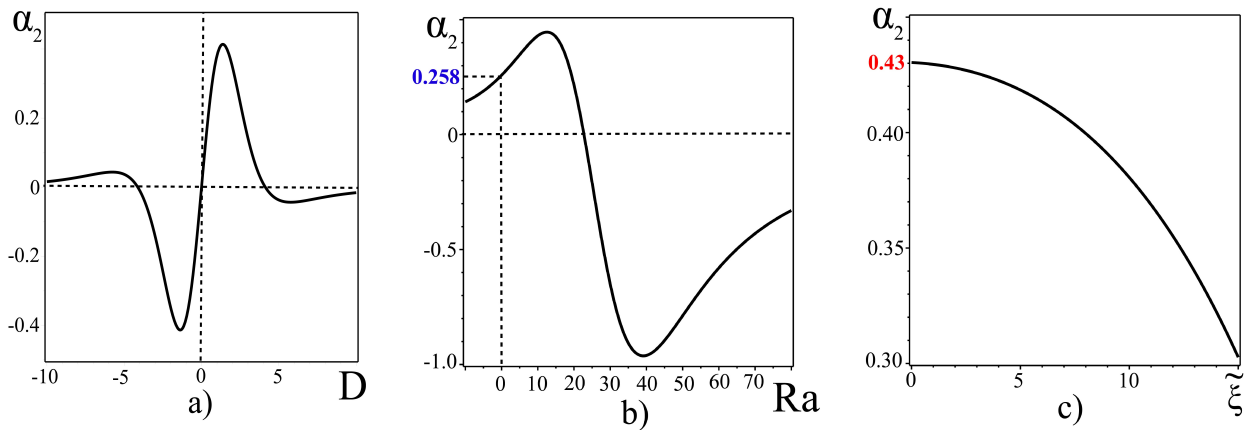
$$\partial_T (\nabla^2_Z W_1 - W_1) - \nabla^4_Z W_1 =$$

$$= \frac{f^2_0}{8} \nabla^3_Z \left[\frac{D^2}{36(1-W_1)^2 + \left[\frac{D^2}{2} + 9 - (1-W_1)^2 \right]^2 + \Xi^{(1)}_1 - \widetilde{\xi}\Xi^{(2)}_1 + \widetilde{\xi}\Xi^{(3)}_1} \right] +$$

$$+ \frac{f^2_0}{2} \nabla^3_Z \left[\frac{D \left(\frac{3}{2} - \frac{1.05 Ra}{17.64 + Pr^2 (1-1.47 W_2)^2} \right)}{36(1-W_2)^2 + \left[\frac{D^2}{2} + 9 - (1-W_2)^2 \right]^2 + \Xi^{(1)}_2 - \widetilde{\xi}\Xi^{(2)}_2 + \widetilde{\xi}\Xi^{(3)}_2} \right], \tag{37}$$

$$\partial_T (\nabla^2_Z W_2 - W_2) - \nabla^4_Z W_2 =$$

$$= \frac{f^2_0}{8} \nabla^3_Z \left[\frac{D^2}{36(1-W_2)^2 + \left[\frac{D^2}{2} + 9 - (1-W_2)^2 \right]^2 + \Xi^{(1)}_2 - \widetilde{\xi}\Xi^{(2)}_2 + \widetilde{\xi}\Xi^{(3)}_2} \right] -$$

$$- \frac{f^2_0}{2} \nabla^3_Z \left[\frac{D \left(\frac{3}{2} - \frac{1.05 Ra}{17.64 + Pr^2 (1-1.47 W_1)^2} \right)}{36(1-W_1)^2 + \left[\frac{D^2}{2} + 9 - (1-W_1)^2 \right]^2 + \Xi^{(1)}_1 - \widetilde{\xi}\Xi^{(2)}_1 + \widetilde{\xi}\Xi^{(3)}_1} \right], \tag{38}$$

where

$$\Xi^{(1)}_{1,2} = Ra(9 + (1-W_{1,2})^2) \cdot \frac{Pr \widetilde{W}_{1,2} \widetilde{\widetilde{W}}_{1,2} - 12.6 + \frac{Ra}{4}}{17.64 + Pr^2 \widetilde{\widetilde{W}}^2_{1,2}}, \quad \widetilde{W}_{1,2} = 1 - W_{1,2}, \quad \widetilde{\widetilde{W}}_{1,2} = 1 - 1.47 W_{1,2},$$

Figure 2. The α-effect's dependence versus a) magnetic parameter D, b) stratification parameter Ra, and c) Nernst parameter $\widetilde{\xi}$.

$$\Xi_{1,2}^{(2)} = \frac{3}{2}D^2 Ra_1 \cdot \frac{25.2\widetilde{W}_{1,2} + Pr(9 - \widetilde{W}_{1,2}^2)\widetilde{\widetilde{W}}_{1,2}}{17.64 + Pr^2 \widetilde{\widetilde{W}}_{1,2}^2}, \quad \Xi_{1,2}^{(3)} = \frac{D^4}{4} \cdot \frac{Ra_1}{17.64 + Pr^2 \widetilde{\widetilde{W}}_{1,2}^2}\left(\frac{9}{4}\widetilde{\xi}Ra_1 - 3Pr\widetilde{\widetilde{W}}_{1,2}\right).$$

As seen from equations (3)-(3), the vortex dynamo effect in a stratified plasma can emerge under the combined influence of an external small-scale helical force and a magnetic field. In the absence of an external magnetic field, even in the presence of turbulence, large-scale perturbations of the electron velocity undergo ordinary viscous damping.

We first address the linear stability of small field perturbations, followed by an analysis of potential stationary structures.

4. LARGE-SCALE INSTABILITY

In this section, we address the stability of small-scale perturbations in both the velocity and magnetic fields. By applying expressions (6) to equations (3), we obtain the following set of linear equations describing the vortex dynamo:

$$\partial_T (\nabla_Z^2 W_1 - W_1) - \nabla_Z^4 W_1 = \alpha_1 \nabla_Z^3 W_1 + \alpha_2 \nabla_Z^3 W_2,$$

$$\partial_T (\nabla_Z^2 W_2 - W_2) - \nabla_Z^4 W_2 = \alpha_1 \nabla_Z^3 W_2 - \alpha_2 \nabla_Z^3 W_1, \tag{39}$$

here,

$$\alpha_1 = \frac{f_0^2}{8}D^2\alpha, \quad \alpha_2 = \frac{f_0^2}{2}D(\alpha\sigma_0 - \alpha_0\sigma_1),$$

$$\alpha_0 = \frac{4}{(D^2 + 16)^2 + 144 + 40a_0 Ra + 4\widetilde{\xi}(m_0 - c_0)},$$

$$\alpha = \frac{32(20 - D^2 + Ra(a_0 - 5b_0) + \frac{\widetilde{\xi}}{2}(d_0 - n_0))}{\left[(D^2 + 16)^2 + 144 + 40a_0 Ra + 4\widetilde{\xi}(m_0 - c_0)\right]^2}.$$

The explicit form of the coefficients $\sigma_0, \sigma_1, a_0, b_0, c_0, d_0, m_0, n_0$ can be found in Appendix C. We seek a solution to the linear system of equations (4) in the form of plane waves with a wave vector K aligned along the Z-axis, i.e.,

$$W_{1,2} = A_{W_{1,2}} \exp(-i\omega T + iKZ) \tag{40}$$

Substituting expression (40) into the system of equations (4), we obtain the corresponding dispersion relation:

$$\left(i\omega(1 + K^2) - K^4 + i\alpha_1 K^3\right)^2 - \alpha_2^2 K^6 = 0 \tag{41}$$

By representing $\omega = \omega_0 + i\Gamma$ in equation (41), we get:

$$\omega_0 = -\frac{\alpha_1 K^3}{1 + K^2}, \quad \Gamma_{1,2} = \frac{\mp\alpha_2 K^3 - K^4}{1 + K^2}. \tag{42}$$

The solutions given by (42) indicate the presence of unstable oscillatory modes associated with large-scale vortex disturbances. It is important to emphasize that, within the framework of linear theory, the coefficients α_1 and α_2 are independent
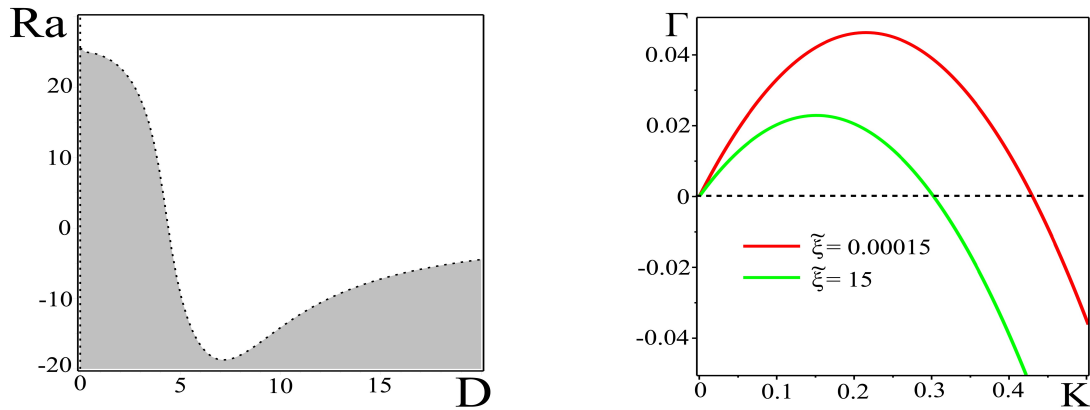
Figure 3. Left: instability region in the (D, Ra) plane (gray: $\alpha_2 > 0$, white: $\alpha_2 < 0$). Right: growth rate $\Gamma(K)$ for $\widetilde{\xi} = 0.00015$ and $\widetilde{\xi} = 15$ at $D = 2$, $Ra = 10$.
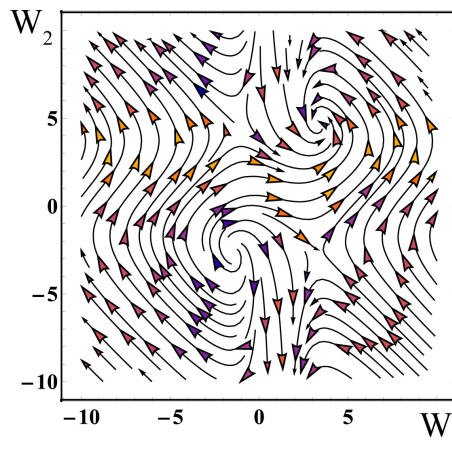
Figure 4. Phase portrait of the dynamical system defined by Eqs. (5)-(5) for $C_5 = -0.005$ and $C_6 = 0.005$.

of the velocity field amplitudes; instead, they depend solely on the magnetic rotation parameter D, the Rayleigh number Ra, the Nernst parameter $\widetilde{\xi}$, and the amplitude of the external forcing f_0. Thus, magnetorotational and thermomagnetic effects may play an important role in the development of large-scale instabilities and the emergence of self-organized structures in stratified magnetized plasma.

We consider the effect of an external magnetic field (characterized by the parameter D) on the gain α_2, which determines the generation of large-scale vortex disturbances. For this analysis, the other parameters are fixed as follows: $f_0 = 10$, $Ra = 5$, $Pr = 1$, $Ra_1 = 0.15$, and $\widetilde{\xi} = 0.15$. Fig. 2a shows that α_2 attains a maximum at a certain value of D. As D increases further, α_2 decreases monotonically, indicating suppression of the α-effect by the magnetic field. Interestingly, the $\alpha_2(D)$ curve also demonstrates that vortex generation can be completely inhibited at specific nonzero values of D, where α_2 vanishes.

Let us now examine how the value of α_2 varies with the plasma heating parameter Ra, while keeping the other parameters fixed: $D = 2$, $Pr = 1$, $Ra_1 = 0.15$, $\widetilde{\xi} = 0.15$, and the amplitude of the external force $f_0 = 10$. The functional dependence $\alpha_2(Ra)$ is presented in Fig. 2b. For $Ra = 0$, the coefficient $\alpha_2 = 0.258$ corresponds to a plasma without a temperature gradient (i.e., no heating). In this regime, the generation of large-scale vortex structures is driven solely by the external helical small-scale forcing and the Lorentz force. As can be seen from Fig. 2b, the presence of thermal stratification ($Ra \neq 0$) can enhance the value of α_2, thereby accelerating the formation of large-scale vortex disturbances compared to the non-stratified case. However, beyond a certain critical value of the stratification parameter Ra_c, the generation process is suppressed, as indicated by $\alpha_2 = 0$. For $Ra > Ra_c$, the sign of the gain coefficient α_2 reverses. As a result, the previously growing mode becomes damped, and vice versa.

In a similar manner, we can examine the influence of the Nernst parameter $\widetilde{\xi}$ on the gain α_2. Fig. 2c clearly shows that the gain coefficient α_2 decreases with increasing $\widetilde{\xi}$, starting from $\alpha_2 \approx 0.43$ at $\widetilde{\xi} = 0$. This reduction can be attributed to the Nernst effect, wherein part of the thermal force is directed perpendicular to both the magnetic field vector $\overline{\mathbf{B}}$ and the temperature gradient $\partial_i T_0$. This transverse component of the thermal force impedes the motion of the electron component

of the plasma, thereby leading to a suppression of the α-effect and a consequent decrease in α_2.

The left part of Fig. 3 shows the combined effect of the external magnetic field and thermal stratification in the (D, Ra) plane. The instability region ($\alpha_2 > 0$) is marked in gray. The right part of Fig. 3 shows the dependence of the growth rate Γ on the wave number K as given by Eq. (42). As the Nernst parameter increases, the instability increment decreases, reflecting the reduction of α_2 with increasing $\widetilde{\xi}$ (see Fig. 2c).

As equations (4) demonstrate, helicity of the small-scale field alone is insufficient for dynamo operation. Efficient generation of large-scale magnetic fields requires some critical parameters to fall within specific ranges, including the external magnetic field parameter D and the thermal driving characterized by the Rayleigh number Ra. Additionally, the geometric configuration plays a crucial role, particularly the vertical upward orientation of the external magnetic field vector $\overline{\mathbf{B}}$.

5. STATIONARY NONLINEAR STRUCTURES

As the large-scale instability develops, the exponential growth of small perturbations $W_{1,2}$ renders the linear approximation invalid. With increasing disturbance amplitude, nonlinear effects become dominant. This leads to a suppression of the nonlinear α-effect coefficients and a transition to a saturated, steady-state regime. In this regime, stable nonlinear vortex and magnetic structures emerge. To identify such stationary structures, we set $\partial_T = 0$ in Eqs. (3)-(3), and perform integration with respect to Z. This procedure yields the following set of nonlinear equations:

$$\frac{dW_1}{dZ} = -\frac{f_0^2}{8} \cdot \frac{D^2}{36(1-W_1)^2 + \left[\frac{D^2}{2} + 9 - (1-W_1)^2\right]^2 + \Xi_1^{(1)} - \widetilde{\xi}\Xi_1^{(2)} + \widetilde{\xi}\Xi_1^{(3)}} -$$

$$-\frac{f_0^2}{2} \cdot \frac{D\left(\frac{3}{2} - \frac{1.05Ra}{17.64+Pr^2(1-1.47W_2)^2}\right)}{36(1-W_2)^2 + \left[\frac{D^2}{2} + 9 - (1-W_2)^2\right]^2 + \Xi_2^{(1)} - \widetilde{\xi}\Xi_2^{(2)} + \widetilde{\xi}\Xi_2^{(3)}} + C_1\frac{Z^2}{2} + C_3 Z + C_5, \qquad (43)$$

$$\frac{dW_2}{dZ} = -\frac{f_0^2}{8} \cdot \frac{D^2}{36(1-W_2)^2 + \left[\frac{D^2}{2} + 9 - (1-W_2)^2\right]^2 + \Xi_2^{(1)} - \widetilde{\xi}\Xi_2^{(2)} + \widetilde{\xi}\Xi_2^{(3)}} +$$

$$+\frac{f_0^2}{2} \cdot \frac{D\left(\frac{3}{2} - \frac{1.05Ra}{17.64+Pr^2(1-1.47W_1)^2}\right)}{36(1-W_1)^2 + \left[\frac{D^2}{2} + 9 - (1-W_1)^2\right]^2 + \Xi_1^{(1)} - \widetilde{\xi}\Xi_1^{(2)} + \widetilde{\xi}\Xi_1^{(3)}} + C_2\frac{Z^2}{2} + C_4 Z + C_6. \qquad (44)$$

Here, the integration constants C_1, C_2, C_3, C_4, C_5, and C_6 are arbitrary. For the purpose of qualitative analysis of Eqs. (5)-(5), the physical parameters are fixed as follows: $f_0 = 1$, $Ra = 5$, $D = 2$, $Pr = 1$, and $\widetilde{\xi} = Ra_1 = 0.15$. To simplify the analysis, we set $C_1 = C_2 = C_3 = C_4 = 0$ and consider the stationary case by equating the left-hand sides of Eqs. (5)-(5) to zero. Under these conditions, the coordinates of the four fixed points $E_{(1,2,3,4)}$ can be determined numerically:

$$E_1(-1.363, 4.68), \ E_2(3.345, -2.635), \ E_3(3.345, 4.646), \ E_4(-1.358, -2.669). \qquad (45)$$

By linearizing the right-hand sides of Eqs. (5)-(5) in the vicinity of the stationary points, we can determine their nature and construct the corresponding phase portrait. This analysis reveals that the system possesses two hyperbolic (saddle) points (E_1, E_2), one stable focus (E_3), and one unstable focus (E_4). The phase portrait of the resulting dynamical system, obtained for the constants $C_5 = -0.005$ and $C_6 = 0.005$, is shown in Fig. 4. The trajectories in the phase space demonstrate characteristic behavior near these points: solutions are repelled from the unstable focus and attracted toward the stable one, while the saddle points form separatrices that partition the phase space into distinct dynamical regions. Physically, these fixed points correspond to stationary nonlinear vortex structures, whose stability or instability determines the long-term evolution of the flow.

The most physically relevant localized solutions correspond to trajectories in the phase portrait that connect stationary points on the phase plane. In particular, the separatrix linking a hyperbolic point to a stable focus represents a solution describing a localized vortex structure, such as a kink with rotational features. An example of such a solution is shown on the left side of Fig. 5, obtained by numerically integrating Eqs. (5)-(5) with the initial conditions $W_1(0) = 3.345$ and $W_2(0) = -2.625$.

Another type of helical kink corresponds to a solution in which the separatrix on the phase plane connects the unstable and stable foci. This solution, shown in the right side of Fig. 5, was obtained by numerically integrating Eqs. (5)-(5) with initial conditions $W_1(0) = 3.345$ and $W_2(0) = 4.63$. All of these solutions – representing large-scale, localized, kink-type vortex structures with rotational features – are generated as a result of the instability mechanisms in the stratified, magnetized plasma with helical force analyzed in this study.

We now turn to the analysis of solutions corresponding to localized magnetic structures. To facilitate this, it is convenient to reformulate the stationary equations for the magnetic field components, Eq. (3), in terms of the current
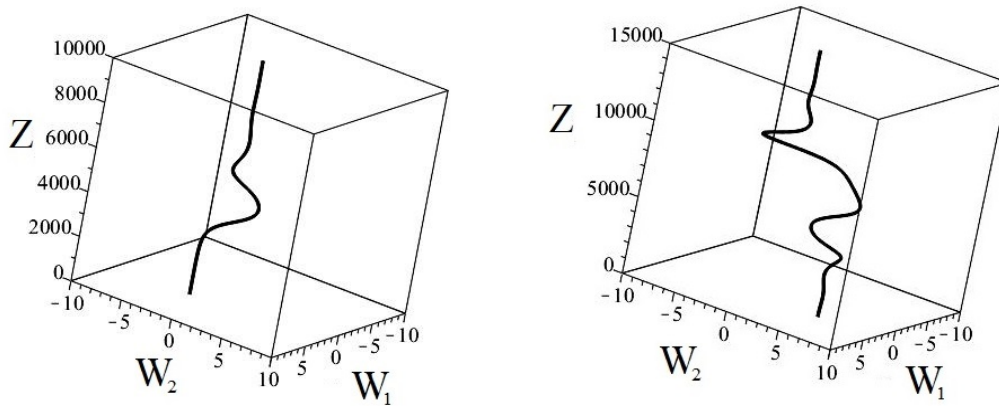
Figure 5. Left: kink-type solution corresponding to a separatrix connecting a hyperbolic point to a stable focus. Right: kink connecting an unstable focus to a stable focus, exhibiting an internal helical structure.

components. This can be done using the relation between the current density and the large-scale electron velocity, $\mathbf{J} = -\mathbf{W}$, together with Ampere's law written as:

$$\frac{dB_2}{dZ} = -J_1, \quad \frac{dB_1}{dZ} = J_2.$$

Substituting these expressions into the stationary equations (3) yields the following system for the current components J_1 and J_2:

$$\frac{dJ_1}{dZ} = \frac{f_0^2}{8} \cdot \frac{D^2}{36(1+J_1)^2 + \left[\frac{D^2}{2} + 9 - (1+J_1)^2\right]^2 + \widetilde{\Xi}_1^{(1)} - \widetilde{\xi}\widetilde{\Xi}_1^{(2)} + \widetilde{\xi}\widetilde{\Xi}_1^{(3)}} +$$

$$+ \frac{f_0^2}{2} \cdot \frac{D\left(\frac{3}{2} - \frac{1.05Ra}{17.64 + Pr^2(1+1.47J_2)^2}\right)}{36(1+J_2)^2 + \left[\frac{D^2}{2} + 9 - (1+J_2)^2\right]^2 + \widetilde{\Xi}_2^{(1)} - \widetilde{\xi}\widetilde{\Xi}_2^{(2)} + \widetilde{\xi}\widetilde{\Xi}_2^{(3)}} + \widetilde{C}_1 Z + \widetilde{C}_3, \tag{46}$$

$$\frac{dJ_2}{dZ} = \frac{f_0^2}{8} \cdot \frac{D^2}{36(1+J_2)^2 + \left[\frac{D^2}{2} + 9 - (1+J_2)^2\right]^2 + \widetilde{\Xi}_2^{(1)} - \widetilde{\xi}\widetilde{\Xi}_2^{(2)} + \widetilde{\xi}\widetilde{\Xi}_2^{(3)}} -$$

$$- \frac{f_0^2}{2} \cdot \frac{D\left(\frac{3}{2} - \frac{1.05Ra}{17.64 + Pr^2(1+1.47J_1)^2}\right)}{36(1+J_1)^2 + \left[\frac{D^2}{2} + 9 - (1+J_1)^2\right]^2 + \widetilde{\Xi}_1^{(1)} - \widetilde{\xi}\widetilde{\Xi}_1^{(2)} + \widetilde{\xi}\widetilde{\Xi}_1^{(3)}} + \widetilde{C}_2 Z + \widetilde{C}_4, \tag{47}$$

where

$$\widetilde{\Xi}_{1,2}^{(1)} = Ra(9 + (1+J_{1,2})^2) \cdot \frac{Pr\widetilde{J}_{1,2}\widetilde{\widetilde{J}}_{1,2} - 12.6 + \frac{Ra}{4}}{17.64 + Pr^2\widetilde{\widetilde{J}}_{1,2}^2}, \quad \widetilde{J}_{1,2} = 1 + J_{1,2}, \quad \widetilde{\widetilde{J}}_{1,2} = 1 + 1.47J_{1,2},$$

$$\widetilde{\Xi}_{1,2}^{(2)} = \frac{3}{2}D^2 Ra_1 \cdot \frac{25.2\widetilde{J}_{1,2} + Pr(9 - \widetilde{J}_{1,2}^2)\widetilde{\widetilde{J}}_{1,2}}{17.64 + Pr^2\widetilde{\widetilde{J}}_{1,2}^2}, \quad \widetilde{\Xi}_{1,2}^{(3)} = \frac{D^4}{4} \cdot \frac{Ra_1}{17.64 + Pr^2\widetilde{\widetilde{J}}_{1,2}^2}\left(\frac{9}{4}\widetilde{\xi}Ra_1 - 3Pr\widetilde{\widetilde{J}}_{1,2}\right).$$

Equations (5)-(5) contain arbitrary integration constants $\widetilde{C}_1$, $\widetilde{C}_2$, $\widetilde{C}_3$, and $\widetilde{C}_4$. To simplify the qualitative analysis, we set $\widetilde{C}_1 = \widetilde{C}_2 = 0$. Under this assumption, we analyze the system by setting the left-hand sides of Eqs. (5)-(5) to zero, which allows us to numerically identify the fixed points and determine their locations in phase space:

$$\widetilde{E}_1(-3.34, 2.635), \quad \widetilde{E}_2(1.363, -4.68), \quad \widetilde{E}_3(1.358, 2.669), \quad \widetilde{E}_4(-3.345, -4.646). \tag{48}$$

As in the case of vortex structures, the system exhibits four stationary points: two hyperbolic points ($\widetilde{E}_1$, $\widetilde{E}_2$), a stable focus ($\widetilde{E}_3$), and an unstable focus ($\widetilde{E}_4$). The corresponding phase portrait of the dynamical system governed by Eqs. (5)-(5), with constants $\widetilde{C}_3 = -0.005$ and $\widetilde{C}_4 = -0.005$, is presented in Fig. 6. Localized magnetic structures naturally correspond to phase trajectories in Fig. 6 that connect equilibrium points in the phase space. The left side of Fig. 7 illustrates such a
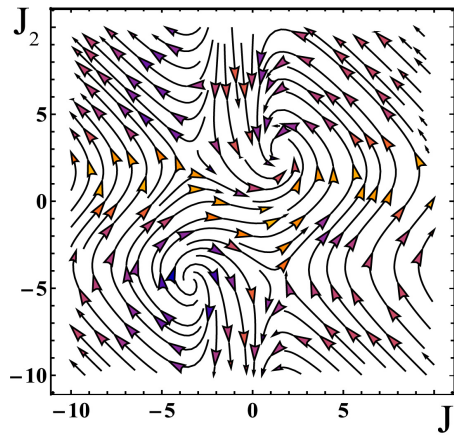
Figure 6. The phase plane of the dynamical system equations (5)-(5) with $\widetilde{C}_3 = -0.005$ and $\widetilde{C}_4 = -0.005$.
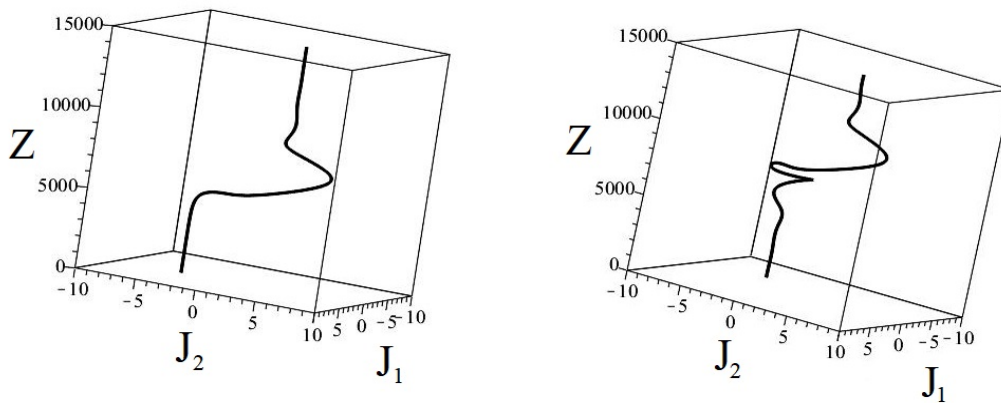
Figure 7. Localized magnetic kink structures analogous to vortex kinks in Fig. 6.

structure in the form of a magnetic kink, obtained through numerical integration of Eqs. (5)-(5) with the initial conditions $J_1(0) = 1.363$ and $J_2(0) = -4.68$. This kink represents a separatrix connecting the hyperbolic point $\widetilde{E}_2$ to the stable focus $\widetilde{E}_3$.

Another type of localized magnetic structure – a spiral kink – is obtained by numerically integrating the system of Eqs.(5)-(5) with initial conditions $J_1(0) = -3.345$ and $J_2(0) = -4.65$. This solution corresponds to a separatrix trajectory on the phase plane that connects the unstable focus $\widetilde{E}_4$ to the stable focus $\widetilde{E}_3$, as shown in the right side of Fig. 7.

As a result of numerically solving the stationary equations (5)-(5) and (5)-(5), we identified localized helical structures of both vortex and magnetic nature.

6. CONCLUSIONS

In this study, a nonlinear dynamo theory has been developed for a fully ionized, temperature-stratified plasma subjected to an external vertical magnetic field and a uniform gravitational field. The plasma dynamics are considered within the framework of electron magnetohydrodynamics (EMHD), assuming immobile and cold ions. The proposed dynamo mechanism incorporates thermomagnetic effects and is based on the α-effect, which arises due to the joint action of a small-scale external helical force and the Lorentz force. The external forcing sustains weak velocity fluctuations in the electron component, forming a low-Reynolds-number turbulence regime ($R \ll 1$). Applying an asymptotic expansion in terms of this small parameter, we derived closed-form equations describing the evolution of large-scale vortex and magnetic perturbations. The linear stage of large-scale instability development was thoroughly analyzed. The regions of instability on the parameter plane (D, Ra), defined by the Lorentz and Rayleigh numbers respectively, were determined. It is shown that the extent and structure of the instability domain are sensitive to the intensity of the small-scale forcing. A key result of this work is the identification of the suppressing role of the Nernst effect on large-scale instability. As the Nernst parameter increases, the growth rate of the instability decreases, owing to the thermomagnetic part of the electron force counteracting the generation process. Conversely, stronger thermal stratification (larger Rayleigh number) enhances the instability until it transitions to convective instability at high values of Ra. In the nonlinear regime, as

the amplitude of perturbations grows, saturation occurs and the system reaches a stationary state. Numerical integration of the nonlinear equations reveals the formation of localized vortex and magnetic structures in the form of spiral kinks. These coherent structures represent the final stage of nonlinear evolution driven by the large-scale dynamo instability in a stratified magnetized plasma.

APPENDIX A. ALGEBRAIC STRUCTURE OF THE ASYMPTOTIC EXPANSIONS

Let us present the algebraic structure of the asymptotic expansion for equations (2)-(18) at different orders in R, starting with the smallest.

At the R^{-3} order, we have just one equation:

$$\partial_i P_{-3} = 0 \quad \Rightarrow \quad P_{-3} = P_{-3}(X) \tag{49}$$

In order R^{-2} we get the equation:

$$\partial_i P_{-2} = 0 \quad \Rightarrow \quad P_{-2} = P_{-2}(X) \tag{50}$$

Equations (49) and (50) are automatically fulfilled as P_{-3} and P_{-2} solely depend on slow variables.

In order R^{-1} we obtain the system of equations:

$$\partial_t W_{-1}^i + W_{-1}^k \partial_k W_{-1}^i = -\partial_i P_{-1} - \nabla_i P_{-3} + \partial_k^2 W_{-1}^i - D\varepsilon_{ijk} W_j e_k + e_i \widetilde{Ra} T_{-1} - W_{-1}^i + \partial_k^2 W_{-1}^i,$$

$$\partial_t T_{-1} - 2.1 Pr^{-1} \partial_k^2 T_{-1} = -1.47 W_{-1}^k \partial_k T_{-1} + W_{-1}^z - \frac{5}{3} Pr^{-1} \xi e_i \varepsilon_{ijk} \partial_i B_0^k, \tag{51}$$

$$\partial_i W_{-1}^i = 0, \qquad \partial_i B_{-1}^i = 0.$$

Upon averaging equations (51) over the "fast" variables, we obtain the secular equations:

$$-\nabla_i P_{-3} - D\varepsilon_{ijk} W_j e_k + e_i \widetilde{Ra} T_{-1} - W_{-1}^i = 0, \quad W_{-1}^z = 0, \tag{52}$$

At zero order R^0, we have:

$$\partial_t v_0^i + W_{-1}^k \partial_k v_0^i = -\partial_i P_0 - \nabla_i P_{-2} - D\varepsilon_{ijk} v_0^j e_k + e_i \widetilde{Ra} T_0 -$$

$$-\widetilde{Ra}_1 \left(0.71 \partial_i T_0 + \frac{3}{2} \widetilde{\xi} D \varepsilon_{ijk} e_j \partial_k T_0 \right) - v_0^i + \partial_k^2 v_0^i + F_0^i,$$

where $\widetilde{Ra}_1 = \widetilde{Ra} \left(\frac{V_{Te}}{g\lambda_0} \right)$ is the modified Rayleigh number,

$$\partial_t T_0 - 2.1 Pr^{-1} \partial_k^2 T_0 = -1.47 W_{-1}^k \partial_k T_0 + v_0^z +$$

$$+\frac{5}{3} Pr^{-1} \xi \partial_i T_0 \varepsilon_{ijk} \partial_j B_0^k - \frac{5}{3} Pr^{-1} \xi e_i \varepsilon_{ijk} (\partial_j B_1^k + \nabla_j B_{-1}^k), \tag{53}$$

$$\partial_t B_0^i = -\varepsilon_{ijk} \partial_j E_0^k, \ \varepsilon_{ijk} \partial_j B_0^k = 0, \ \partial_i v_0^i = 0, \ \partial_i B_0^i = 0.$$

These equations give secular terms:

$$\nabla P_{-2} = 0 \quad \Rightarrow \quad P_{-2} = \text{const}, \ (\nabla \times \mathbf{B}_{-1})_z = 0.$$

Let us look at the first-order approximation R^1:

$$\partial_t v_1^i + W_{-1}^k \partial_k v_1^i + v_0^k \partial_k v_0^i + W_{-1}^k \nabla_k W_{-1}^i = -\nabla_i P_{-1} -$$

$$-\partial_i \left(P_1 + \overline{P}_1 \right) - E_{-1}^i - D\varepsilon_{ijk} v_1^j e_k - \varepsilon_{ijk} W_{-1}^j B_{-1}^k + e_i \widetilde{Ra} T_1 -$$

$$-\widetilde{Ra}_1 \left(0.71(\partial_i T_1 + \nabla_i T_{-1}) + \frac{3}{2} \widetilde{\xi} D\varepsilon_{ijk} e_j (\partial_k T_1 + \nabla_k T_{-1}) \right) - v_1^i + \partial_k^2 v_1^i + 2\partial_k \nabla_k W_{-1}^i,$$

$$\partial_t T_1 - 2.1 Pr^{-1} \partial_k^2 T_1 - 4.2 Pr^{-1} \partial_k \nabla_k T_{-1} = -1.47(W_{-1}^k \partial_k T_1 + W_{-1}^k \nabla_k T_{-1} + v_0^k \partial_k T_0) + v_z +$$

$$+\frac{5}{3} Pr^{-1} \xi \varepsilon_{ijk} (\partial_i T_0 (\partial_j B_1^k + \nabla_j B_{-1}^k) + \partial_i T_1 \partial_j B_0^k) - \frac{5}{3} Pr^{-1} \xi e_i \varepsilon_{ijk} \partial_j B_2^k, \tag{54}$$

$$\partial_t B_1^i = -\varepsilon_{ijk} (\partial_j E_1^k + \nabla_j E_{-1}^k), \ \varepsilon_{ijk} (\partial_j B_1^k + \nabla_j B_{-1}^k) = -W_{-1}^i,$$

$$\partial_i v_1^i + \nabla_i W_{-1}^i = 0, \quad \partial_i B_1^i + \nabla_i B_{-1}^i = 0.$$

From this system of equations, secular equations are derived in the form

$$W_{-1}^k \nabla_k W_{-1}^i = -\nabla_i P_{-1} - E_{-1}^i - \varepsilon_{ijk} W_{-1}^j B_{-1}^k - \widetilde{Ra}_1 \left(0.71\nabla_i T_{-1} + \frac{3}{2}\widetilde{\xi}D\varepsilon_{ijk}e_j\nabla_k T_{-1}\right), \tag{55}$$

$$\varepsilon_{ijk}\nabla_j E_{-1}^k = 0, \quad \varepsilon_{ijk}\nabla_j B_{-1}^k = -W_{-1}^i, \tag{56}$$

$$W_{-1}^k \nabla_k T_{-1} = 0, \quad \nabla_i W_{-1}^i = 0, \quad \nabla_i B_{-1}^i = 0. \tag{57}$$

At second order R^2, we get

$$\partial_t v_2^i + W_{-1}^k \partial_k v_2^i + v_0^k \partial_k v_1^i + W_{-1}^k \nabla_k v_0^i + v_0^k \nabla_k W_{-1}^i + v_1^k \partial_k v_0^i =$$

$$= -\partial_i P_2 - \nabla_i P_0 - E_0^i - D\varepsilon_{ijk}v_2^j e_k - \varepsilon_{ijk}v_0^j B_{-1}^k + e_i\widetilde{Ra}T_2 -$$

$$-\widetilde{Ra}_1\left(0.71\partial_i T_2 + \frac{3}{2}\widetilde{\xi}D\varepsilon_{ijk}e_j\partial_k T_2\right) - v_2^i + \partial_k^2 v_2^i + 2\partial_k\nabla_k v_0^i,$$

$$\partial_t T_2 - 2.1Pr^{-1}\partial_k^2 T_2 - 4.2Pr^{-1}\partial_k\nabla_k T_0 = -1.47(W_{-1}^k\partial_k T_2 +$$

$$+W_{-1}^k\nabla_k T_0 + v_0^k\partial_k T_1 + v_0^k\nabla_k T_{-1} + v_1^k\partial_k T_0) + v_2^z + \frac{5}{3}Pr^{-1}\xi\varepsilon_{ijk}\times$$

$$\times(\partial_i T_0\partial_j B_2^k + \partial_i T_1(\partial_j B_1^k + \nabla_j B_{-1}^k) + \partial_i T_2\partial_j B_0^k) -$$

$$-\frac{5}{3}Pr^{-1}\xi e_i\varepsilon_{ijk}(\partial_j B_3^k + \nabla_j B_1^k), \tag{58}$$

$$\partial_t B_2^i = -\varepsilon_{ijk}\partial_j E_2^k, \quad \varepsilon_{ijk}\partial_j B_2^k = -v_0^i,$$

$$\partial_i v_2^i + \nabla_i v_0^i = 0, \quad \partial_i B_2^i + \nabla_i B_0^i = 0.$$

The system (6) is averaged over the fast variables, and no secular terms of order R^2 are found. Finally, the order R^3 is reached, where the equations are

$$\partial_t v_3^i + \partial_T W_{-1}^i + W_{-1}^k\partial_k v_3^i + v_0^k\partial_k v_2^i + W_{-1}^k\nabla_k v_1^i + v_0^k\nabla_k v_0^i +$$

$$+v_1^k\partial_k v_1^i + v_1^k\nabla_k W_{-1}^i + v_2^k\partial_k v_0^i = -\partial_i P_3 - \nabla_i\left(P_1 + \overline{P}_1\right) -$$

$$-\left(E_1^i + \overline{E}_1^i\right) - D\varepsilon_{ijk}v_3^j e_k - \varepsilon_{ijk}W_{-1}^j B_1^k - \varepsilon_{ijk}v_1^j B_{-1}^k + e_i\widetilde{Ra}T_3 -$$

$$-\widetilde{Ra}_1\left(0.71(\partial_i T_3 + \nabla_i T_1) + \frac{3}{2}\widetilde{\xi}D\varepsilon_{ijk}e_j(\partial_k T_3 + \nabla_k T_1)\right) - v_3^i + \partial_k^2 v_3^i + 2\partial_k\nabla_k v_1^i + \nabla_k^2 W_{-1}^i,$$

$$\partial_t T_3 + \partial_T T_{-1} - 2.1Pr^{-1}(\partial_k^2 T_3 + 2\partial_k\nabla_k T_1 + \nabla^2 T_{-1}) =$$

$$= -1.47(W_{-1}^k\partial_k T_3 + W_{-1}^k\nabla_k T_1 + v_0^k\partial_k T_2 + v_0^k\nabla_k T_0 + v_1^k\nabla_k T_1 +$$

$$+v_1^k\nabla_k T_{-1} + v_2^k\partial_k T_0) + v_3^z + \frac{5}{3}Pr^{-1}\xi\varepsilon_{ijk}(\partial_i T_0(\partial_j B_3^k + \nabla_j B_1^k) +$$

$$+\partial_i T_1\partial_j B_2^k + \partial_i T_2(\partial_j B_1^k + \nabla_j B_{-1}^k) + \partial_i T_3\partial_j B_0^k) - \frac{5}{3}Pr^{-1}\xi e_i\varepsilon_{ijk}\nabla_j B_2^k, \tag{59}$$

$$\partial_t B_3^i + \partial_T B_{-1}^i = -\varepsilon_{ijk}(\partial_j E_3^k + \nabla_j E_1^k),$$

$$\varepsilon_{ijk}(\partial_j B_3^k + \nabla_j B_1^k) = -v_1^i,$$

$$\partial_i v_3^i + \nabla_i v_1^i = 0, \quad \partial_i B_3^i + \nabla_i B_1^i = 0.$$

The fundamental secular equations that describe the development of large-scale disturbances in a stratified plasma with a vertical external magnetic field are obtained by averaging this system of equations over fast variables:

$$\partial_T W_{-1}^i + \nabla_k\left(\overline{v_0^k v_0^i}\right) = -\nabla_i\overline{P}_1 - \overline{E}_1^i + \nabla_k^2 W_{-1}^i, \tag{60}$$

$$\partial_T T_{-1} - 2.1Pr^{-1}\nabla^2 T_{-1} = -1.47\nabla_k\left(\overline{v_0^k T_0}\right), \tag{61}$$

$$\partial_T B_{-1}^i = -\varepsilon_{ijk}\nabla_j\overline{E}_1^k. \tag{62}$$

APPENDIX B. SMALL-SCALE FIELDS

Let us now examine the zero-order equations in R, presented in Appendix A (see Eq. (6)). By introducing the differential operators

$$\widehat{D}_W = \partial_t + 1 - \partial^2 + W_{-1}^k \partial_k, \quad \widehat{D}_T = \partial_t + 1.47 W_{-1}^k \partial_k - 2.1 Pr^{-1} \partial^2, \tag{63}$$

the system (6) can be conveniently rewritten in the following form:

$$\widehat{D}_W v_0^i = -\partial_i P_0 - D\varepsilon_{ijk} v_0^j e_k + e_i \widetilde{Ra} T_0 - \widetilde{Ra}_1 \left(0.71 \partial_i T_0 + \frac{3}{2} \widetilde{\xi} D \varepsilon_{ijk} e_j \partial_k T_0 \right) + F_0^i \tag{64}$$

$$\widehat{D}_T T_0 = e_k v_0^k \tag{65}$$

$$\partial_i v_0^i = \partial_k B_0^k = \partial_i F_0^i = 0 \tag{66}$$

By substituting Eq. (65) into Eq. (64) and applying the solenoidality condition for the fields (Eq. (66)), we obtain the following expression for the pressure P_0:

$$P_0 = \widehat{P}_1 u_0 + \widehat{P}_2 v_0 + \widehat{P}_3 w_0 \tag{67}$$

where

$$v_0^x = u_0, v_0^y = v_0, v_0^z = w_0,$$

$$\widehat{P}_1 = \frac{D\partial_y}{\partial^2}, \ \widehat{P}_2 = -\frac{D\partial_x}{\partial^2}, \ \widehat{P}_3 = \widetilde{Ra} \frac{\partial_z}{\widehat{D}_T \partial^2} - 0.71 \frac{\widetilde{Ra}_1}{\widehat{D}_T}.$$

Utilizing the representation given in Eq. (67), the pressure term in Eqs. (64) can be eliminated, yielding the system of equations that governs the velocity fields in the zeroth-order approximation:

$$\begin{cases} \left(\widehat{D}_W + \widehat{p}_{1x} \right) u_0 + \left(\widehat{p}_{2x} + D \right) v_0 + \left(\widehat{p}_{3x} + \widehat{D}_{Rx} \right) w_0 = F_0^x, \\ \left(\widehat{p}_{1y} - D \right) u_0 + \left(\widehat{D}_W + \widehat{p}_{2y} \right) v_0 + \left(\widehat{p}_{3y} + \widehat{D}_{Ry} \right) w_0 = F_0^y, \\ \widehat{p}_{1z} u_0 + \widehat{p}_{2z} v_0 + \left(\widehat{D}_W + \widehat{p}_{3z} - \frac{\widetilde{Ra}}{\widehat{D}_T} + \widehat{D}_{Rz} \right) w_0 = 0, \end{cases} \tag{68}$$

where

$$\widehat{D}_{Rx} = \frac{\widetilde{Ra}_1}{\widehat{D}_T} \left(0.71 \partial_x - \frac{3}{2} \widetilde{\xi} D \partial_y \right), \ \widehat{D}_{Ry} = \frac{\widetilde{Ra}_1}{\widehat{D}_T} \left(0.71 \partial_y + \frac{3}{2} \widetilde{\xi} D \partial_x \right), \ \widehat{D}_{Rz} = 0.71 \widetilde{Ra}_1 \frac{\partial_z}{\widehat{D}_T},$$

$$\widehat{p}_{1x} = \partial_x P_1, \quad \widehat{p}_{2x} = \partial_x P_2, \quad \widehat{p}_{3x} = \partial_x P_3, \ \widehat{p}_{1y} = \partial_y P_1, \quad \widehat{p}_{2y} = \partial_y P_2, \quad \widehat{p}_{3y} = \partial_y P_3,$$

$$\widehat{p}_{1z} = \partial_z P_1, \quad \widehat{p}_{2z} = \partial_z P_2, \quad \widehat{p}_{3z} = \partial_z P_3.$$

The solution of the system of equations (68) can be obtained by applying Cramer's rule:

$$u_0 = \frac{1}{\Delta} \left(\widehat{d}_1 \cdot F_0^x + \widehat{d}_2 \cdot F_0^y \right), \ v_0 = \frac{1}{\Delta} \left(\widehat{d}_3 \cdot F_0^x + \widehat{d}_4 \cdot F_0^y \right), \ w_0 = \frac{1}{\Delta} \left(\widehat{d}_5 \cdot F_0^x + \widehat{d}_6 \cdot F_0^y \right). \tag{69}$$

where

$$\widehat{d}_1 = \left(\widehat{D}_W + \widehat{p}_{2y} \right) \left(\widehat{D}_W + \widehat{p}_{3z} - \frac{\widetilde{Ra}}{\widehat{D}_T} + \widehat{D}_{Rz} \right) - \widehat{p}_{2z} \left(\widehat{p}_{3y} + \widehat{D}_{Ry} \right),$$

$$\widehat{d}_2 = \left(\widehat{p}_{3x} + \widehat{D}_{Rx} \right) \widehat{p}_{2z} - \left(\widehat{p}_{2x} + D \right) \left(\widehat{D}_W + \widehat{p}_{3z} - \frac{\widetilde{Ra}}{\widehat{D}_T} + \widehat{D}_{Rz} \right),$$

$$\widehat{d}_3 = \left(\widehat{p}_{3y} + \widehat{D}_{Ry} \right) \widehat{p}_{1z} - \left(\widehat{p}_{1y} - D \right) \left(\widehat{D}_W + \widehat{p}_{3z} - \frac{\widetilde{Ra}}{\widehat{D}_T} + \widehat{D}_{Rz} \right),$$

$$\widehat{d}_4 = \left(\widehat{D}_W + \widehat{p}_{1x} \right) \left(\widehat{D}_W + \widehat{p}_{3z} - \frac{\widetilde{Ra}}{\widehat{D}_T} + \widehat{D}_{Rz} \right) - \left(\widehat{p}_{3x} + \widehat{D}_{Rx} \right) \widehat{p}_{1z},$$

$$\widehat{d}_5 = \left(\widehat{p}_{1y} - D \right) \widehat{p}_{2z} - \left(\widehat{D}_W + \widehat{p}_{2y} \right) \widehat{p}_{1z}, \ \widehat{d}_6 = \left(\widehat{p}_{2x} + D \right) \widehat{p}_{1z} - \left(\widehat{D}_W + \widehat{p}_{1x} \right) \widehat{p}_{2z}.$$

Here, the symbol Δ denotes the determinant of the system of equations (68):

$$\Delta = \left(\widehat{D}_W + \widehat{p}_{1x} \right) \cdot \widehat{d}_1 + \left(\widehat{p}_{2x} + D \right) \cdot \widehat{d}_3 + \left(\widehat{p}_{3x} + \widehat{D}_{Rx} \right) \cdot \widehat{d}_5. \tag{70}$$

All operators involved in (69)-(70) are mutually commutative, which simplifies the evaluation of these expressions. To compute expressions (69)-(70), we rewrite the external force (12) in complex form:

$$\mathbf{F}_0 = \mathbf{i}\,\frac{f_0}{2}\,e^{i\phi_2} + \mathbf{j}\,\frac{f_0}{2}e^{i\phi_1} + c.c. \tag{71}$$

It follows from substituting (71) into (69)-(70) that the operators act on the exponential term from the left, such that $\widehat{p}\exp(i\mathbf{kx} - i\omega_0 t) = \exp(i\mathbf{kx} - i\omega_0 t)p(\mathbf{k}, -\omega_0)$. Therefore, we make use of the following properties of the eigenfunctions $p(\mathbf{k}, -\omega_0)$:

$$\widehat{D}_{W,T}e^{i\phi_1} = e^{i\phi_1}D_{W,T}\left(\mathbf{k}_1, -\omega_0\right), \;\; \widehat{D}_{W,T}e^{i\phi_2} = e^{i\phi_2}D_{W,T}\left(\mathbf{k}_2, -\omega_0\right),$$

$$\Delta e^{i\phi_1} = e^{i\phi_1}\Delta\left(\mathbf{k}_1, -\omega_0\right), \;\; \Delta e^{i\phi_2} = e^{i\phi_2}\Delta\left(\mathbf{k}_2, -\omega_0\right). \tag{72}$$

To simplify the formulas, let us set $k_0 = 1$ and $\omega_0 = 1$, introducing new designations:

$$D_W\left(\mathbf{k}_1, -\omega_0\right) = D_{W_1}^* = 3 - i\left(1 - W_1\right),$$

$$D_W\left(\mathbf{k}_2, -\omega_0\right) = D_{W_2}^* = 3 - i\left(1 - W_2\right),$$

$$D_T\left(\mathbf{k}_1, -\omega_0\right) = D_{T_1}^* = 4.2Pr^{-1} - i\left(1 - 1.47W_1\right),$$

$$D_T\left(\mathbf{k}_2, -\omega_0\right) = D_{T_2}^* = 4.2Pr^{-1} - i\left(1 - 1.47W_2\right). \tag{73}$$

$$\Delta\left(\mathbf{k}_1, -\omega_0\right) = \Delta_1^* = D_{W_1}^*\left(D_{W_1}^*\left(D_{W_1}^* - \frac{\widetilde{Ra}}{2D_{T_1}^*}\right) + \frac{D^2}{2}\left(1 + \frac{3}{2}\widetilde{\xi}\frac{i\widetilde{Ra}_1}{D_{T_1}^*}\right)\right),$$

$$\Delta\left(\mathbf{k}_2, -\omega_0\right) = \Delta_2^* = D_{W_2}^*\left(D_{W_2}^*\left(D_{W_2}^* - \frac{\widetilde{Ra}}{2D_{T_2}^*}\right) + \frac{D^2}{2}\left(1 + \frac{3}{2}\widetilde{\xi}\frac{i\widetilde{Ra}_1}{D_{T_2}^*}\right)\right).$$

Here and throughout the text, the superscript * denotes complex conjugation. Based on formulas (6), we can determine the zeroth-order approximation of the velocity field:

$$u_0 = e^{i\phi_2}\frac{f_0}{2}\frac{A_2^*}{D_{W_2}^*A_2^* + \frac{D^2}{2}B_2^*} - e^{i\phi_1}\frac{f_0}{2}\frac{D/2}{D_{W_1}^*A_1^* + \frac{D^2}{2}B_1^*} + c.c. =$$

$$= u_{01}e^{i\phi_1} + u_{02}e^{-i\phi_1} + u_{03}e^{i\phi_2} + u_{04}e^{-i\phi_2}, \tag{74}$$

$$v_0 = e^{i\phi_2}\frac{f_0}{2}\frac{D/2}{D_{W_2}^*A_2^* + \frac{D^2}{2}B_2^*} + e^{i\phi_1}\frac{f_0}{2}\frac{A_1^*}{D_{W_1}^*A_1^* + \frac{D^2}{2}B_1^*} + c.c. =$$

$$= v_{01}e^{i\phi_1} + v_{02}e^{-i\phi_1} + v_{03}e^{i\phi_2} + v_{04}e^{-i\phi_2}, \tag{75}$$

$$w_0 = e^{i\phi_1}\frac{f_0}{2}\frac{D/2}{D_{W_1}^*A_1^* + \frac{D^2}{2}B_1^*} - e^{i\phi_2}\frac{f_0}{2}\frac{D/2}{D_{W_2}^*A_2^* + \frac{D^2}{2}B_2^*} + c.c. =$$

$$= w_{01}e^{i\phi_1} + w_{02}e^{-i\phi_1} + w_{03}e^{i\phi_2} + w_{04}e^{-i\phi_2}, \tag{76}$$

where

$$A_{1,2}^* = D_{W_{1,2}}^* - \frac{\widetilde{Ra}}{2D_{T_{1,2}}^*}, \;\; B_{1,2}^* = 1 + \frac{3}{2}\widetilde{\xi}\frac{i\widetilde{Ra}_1}{D_{T_{1,2}}^*}. \tag{77}$$

The indices $(1, 2)$ in the expressions for A, B are written in accordance with the components W_1 and W_2. The following relationships are satisfied between the velocity components:

$$u_{02} = \left(u_{01}\right)^*, \;\; u_{04} = \left(u_{03}\right)^*, \;\; v_{02} = \left(v_{01}\right)^*, \;\; v_{04} = \left(v_{03}\right)^*, \;\; w_{02} = \left(w_{01}\right)^*, \;\; w_{04} = \left(w_{03}\right)^*.$$

APPENDIX C. CALCULATIONS OF THE REYNOLDS STRESSES

In order to close the system of equations (30)-(31) governing the evolution of large-scale velocity fields $\mathbf{W}_{-1}$, it is essential to compute correlators of the following form:

$$T^{31} = \overline{w_0 u_0} = \overline{w_{01}(u_{01})^*} + \overline{(w_{01})^* u_{01}} + \overline{w_{03}(u_{03})^*} + \overline{(w_{03})^* u_{03}} \tag{78}$$

$$T^{32} = \overline{w_0 v_0} = \overline{w_{01}(v_{01})^*} + \overline{(w_{01})^* v_{01}} + \overline{w_{03}(v_{03})^*} + \overline{(w_{03})^* v_{03}} \tag{79}$$

Substituting the expressions for the small-scale velocity fields (6)-(6) into the definitions (78)-(79) yields the following:

$$T^{31} = -\frac{f_0^2}{8} \frac{D(A_2 + A_2^*)}{\left| D_{W_2} A_2 + \frac{D^2}{2} B_2 \right|^2} - \frac{f_0^2}{8} \frac{D^2}{\left| D_{W_1} A_1 + \frac{D^2}{2} B_1 \right|^2}, \tag{80}$$

$$T^{32} = -\frac{f_0^2}{8} \frac{D(A_1 + A_1^*)}{\left| D_{W_1} A_1 + \frac{D^2}{2} B_1 \right|^2} - \frac{f_0^2}{8} \frac{D^2}{\left| D_{W_2} A_2 + \frac{D^2}{2} B_2 \right|^2}. \tag{81}$$

Using the expressions given in (77), we derive a set of useful relations for calculating T^{31} and T^{32} as follows:

$$\left| D_{W_{1,2}} \right|^2 = D_{W_{1,2}} D_{W_{1,2}}^* = 9 + (1 - W_{1,2})^2 = 9 + \widetilde{W}_{1,2}^2, \; \left| D_{T_{1,2}} \right|^2 = D_{T_{1,2}} D_{T_{1,2}}^* =$$

$$= 17.64 Pr^{-2} + (1 - 1.47 W_{1,2})^2 = 17.64 Pr^{-2} + \widetilde{\widetilde{W}}_{1,2}^2,$$

$$\left| A_{1,2} \right|^2 = A_{1,2} A_{1,2}^*, \; \left| A_{1,2} \right|^2 = 9 + \widetilde{W}_{1,2}^2 + \frac{Ra}{17.64 + Pr^2 \widetilde{\widetilde{W}}_{1,2}^2} \left(Pr \widetilde{W}_{1,2} \widetilde{\widetilde{W}}_{1,2} - 12.6 + \frac{Ra}{4} \right),$$

$$\left| B_{1,2} \right|^2 = B_{1,2} B_{1,2}^*, \; \left| B_{1,2} \right|^2 = 1 + \frac{\widetilde{\xi} Ra_1}{17.64 + Pr^2 \widetilde{\widetilde{W}}_{1,2}^2} \left(\frac{9}{4} \widetilde{\xi} Ra_1 - 3 Pr \widetilde{\widetilde{W}}_{1,2} \right),$$

$$A_{1,2} + A_{1,2}^* = 6 - \frac{4.2 Ra}{17.64 + Pr^2 \widetilde{\widetilde{W}}_{1,2}^2}, \quad \Pi_{1,2} = \left| D_{W_{1,2}} A_{1,2} + \frac{D^2}{2} B_{1,2} \right|^2 =$$

$$= 36(1 - W_{1,2})^2 + \left[\frac{D^2}{2} + 9 - (1 - W_{1,2})^2 \right]^2 + \Xi_{1,2}^{(1)} - \widetilde{\xi} \Xi_{1,2}^{(2)} + \widetilde{\xi} \Xi_{1,2}^{(3)},$$

$$\Xi_{1,2}^{(1)} = Ra(9 + (1 - W_{1,2})^2) \cdot \frac{Pr \widetilde{W}_{1,2} \widetilde{\widetilde{W}}_{1,2} - 12.6 + \frac{Ra}{4}}{17.64 + Pr^2 \widetilde{\widetilde{W}}_{1,2}^2},$$

$$\Xi_{1,2}^{(2)} = \frac{3}{2} D^2 Ra_1 \cdot \frac{25.2 \widetilde{W}_{1,2} + Pr(9 - \widetilde{W}_{1,2}^2) \widetilde{\widetilde{W}}_{1,2}}{17.64 + Pr^2 \widetilde{\widetilde{W}}_{1,2}^2}, \; \Xi_{1,2}^{(3)} = \frac{D^4}{4} \cdot \frac{Ra_1}{17.64 + Pr^2 \widetilde{\widetilde{W}}_{1,2}^2} \left(\frac{9}{4} \widetilde{\xi} Ra_1 - 3 Pr \widetilde{\widetilde{W}}_{1,2} \right).$$

Substituting the above relations into (80)-(81), we derive the general form of the Reynolds stress expressions:

$$T^{31} = -\frac{f_0^2}{8} \frac{D^2}{\Pi_1} - \frac{f_0^2}{2} \frac{D}{\Pi_2} \left(\frac{3}{2} - \frac{1.05 Ra}{17.64 + Pr^2(1 - 1.47 W_2)^2} \right),$$

$$T^{32} = -\frac{f_0^2}{8} \frac{D^2}{\Pi_2} + \frac{f_0^2}{2} \frac{D}{\Pi_1} \left(\frac{3}{2} - \frac{1.05 Ra}{17.64 + Pr^2(1 - 1.47 W_1)^2} \right). \tag{82}$$

At small $W_{1,2}$, module $\Pi_{1,2}$ can be expanded into a series in $W_{1,2}$:

$$\Pi_{1,2}^{-1} \approx \alpha_0 + \alpha W_{1,2}, \; \alpha_0 = \frac{4}{(D^2 + 16)^2 + 144 + 40 a_0 Ra + 4 \widetilde{\xi}(m_0 - c_0)},$$

$$\alpha = \frac{32(20 - D^2 + Ra(a_0 - 5 b_0) + \frac{\widetilde{\xi}}{2}(d_0 - n_0))}{\left[(D^2 + 16)^2 + 144 + 40 a_0 Ra + 4 \widetilde{\xi}(m_0 - c_0) \right]^2}, \tag{83}$$

where

$$a_0 = \frac{Pr - 12.6 + Ra/4}{17.64 + Pr^2}, \; b_0 = \frac{2.94Pr^2(Pr - 12.6 + Ra/4)}{(17.64 + Pr^2)^2} - \frac{2.47Pr}{17.64 + Pr^2},$$

$$c_0 = \frac{3}{2}D^2 Ra_1 \cdot \frac{25.2 + 8Pr}{17.64 + Pr^2}, \; d_0 = \frac{3}{2}D^2 Ra_1 \cdot \left[\frac{2.94Pr^2(25.2 + 8Pr)}{(17.64 + Pr^2)^2} - \frac{25.2 + 9.76Pr}{17.64 + Pr^2} \right],$$

$$m_0 = \frac{D^4}{4} Ra_1 \cdot \frac{\frac{9}{4}\widetilde{\xi}Ra_1 - 3Pr}{17.64 + Pr^2}, \; n_0 = \frac{D^4}{4} Ra_1 \cdot \left[\frac{4.41Pr}{17.64 + Pr^2} + \frac{2.94Pr^2\left(\frac{9}{4}\widetilde{\xi}Ra_1 - 3Pr\right)}{(17.64 + Pr^2)^2} \right].$$

At small values of $W_{1.2}$, the Reynolds stresses given in (6) take the following form:

$$T^{31} \approx -\frac{f_0^2}{8}D^2(\alpha_0 + \alpha W_1) - \frac{f_0^2}{2}D(\alpha_0\sigma_0 + (\alpha\sigma_0 - \alpha_0\sigma_1)W_2),$$

$$T^{32} \approx -\frac{f_0^2}{8}D^2(\alpha_0 + \alpha W_2) + \frac{f_0^2}{2}D(\alpha_0\sigma_0 + (\alpha\sigma_0 - \alpha_0\sigma_1)W_1), \tag{84}$$

$$\sigma_0 = \frac{3}{2} - \frac{1.05Ra}{17.64 + Pr^2}, \; \sigma_1 = \frac{3.087RaPr^2}{(17.64 + Pr^2)^2}.$$

Expression (6) for the coefficient of the α-effect shows great similarity to the previously obtained results for a rotating viscous fluid [16], the key difference being that the parameter D is due to the Lorentz force rather than the Coriolis force as in Ref. [16].

ORCID

Michael I. Kopp, https://orcid.org/0000-0001-7457-3272; **Volodymyr V. Yanovsky**, https://orcid.org/0000-0003-0461-749X

REFERENCES

[1] G. Moffatt, *Magnetic Field Generation in Electrically Conducting Fluids*, (Cambridge University Press, Cambridge, 1978).

[2] F. Krauze, and K.H. Rädler, *Mean-field Magnetohydrodynamics and Dynamo Theory*, (Pergamon Press, Oxford, 1980).

[3] Ya. Zeldovich, A. Ruzmaikin, and D. Sokoloff, *Magnetic Fields in Astrophysics*, (Gordon and Breach, New York, 1983).

[4] A. Tur, and V. Yanovsky, *Coherent Vortex Structures in Fluids and Plasmas*, (Springer, New York, 2017).

[5] F. Rincon, "Dynamo theories,— J. Plasma Phys. **85**, 205850401 (2019). https://doi.org/10.1017/S0022377819000539

[6] S.M. Tobias, "The turbulent dynamo," J. Fluid Mech. **912**, P1 (2021). https://doi.org/10.1017/jfm.2020.1076

[7] V. Urpin, "Nernst effect and generation of magnetic field in radiation-heated plasma," Plasma Phys. Rep. 45, 366–371 (2019). https://doi.org/10.1134/S1063780X19030103

[8] V. Urpin, "Thermal generation of the magnetic field in the surface layers of massive stars," Mon. Not. R. Astron. Soc. **472**, L5–L9 (2017). https://doi.org/10.1093/mnrasl/slx127

[9] M.I. Kopp, A.V. Tur, and V.V. Yanovsky, "Spontaneous generation of magnetic fields in thin layers of stratified plasma," Phys. Plasmas, **29**, 042115 (2022). https://doi.org/10.1063/5.0087543

[10] A. Schlüter, and L. Biermann, "Über den Ursprung der Magnetfelder auf Sternen und im interstellaren Raum," Z. Naturforsch. A, **5**, 65 (1950). https://doi.org/10.1515/zna-1950-0201

[11] M.I. Kopp, and V.V. Yanovsky, "Features of generation of spontaneous magnetic fields in fully ionized plasma," Probl. At. Sci. Technol. 154(6), 25–30 (2024).

[12] V.P. Lakhin, and T.J. Schep, "On the generation of mean fields by small-scale electron magnetohydrodynamic turbulence," Phys. Plasmas, **11**, 1424–1439 (2004). https://doi.org/10.1063/1.1645275

[13] U. Frisch, Z.S. She, and P.L. Sulem, "Large scale flow driven by the anisotropic kinetic alpha effect," Physica D, **28**, 382–392 (1987). https://doi.org/10.1016/0167-2789(87)90026-1

[14] P.L. Sulem, Z.S. She, H. Scholl, and U. Frisch, "Generation of large-scale structures in three-dimensional flow lacking parity-invariance," J. Fluid Mech. **205**, 341–358 (1989). https://doi.org/10.1017/S0022112089002086

[15] B. Dubrulle, and U. Frisch, "Eddy viscosity of parity-invariant flow," Phys. Rev. A, **43**, 5355–5364 (1991). https://doi.org/10.1103/PhysRevA.43.5355

[16] M.I. Kopp, and V.V. Yanovsky, "Vortex Dynamo in Rotating Media," East Eur. J. Phys. (2), 7–50 (2023). https://doi.org/10.26565/2312-4334-2023-2-01

[17] M.I. Kopp, A.V. Tur, and V.V. Yanovsky, "Large-scale convective instability in an electroconducting medium with small-scale helicity," JETP, **120**(4), 733–750 (2015). https://doi.org/10.1134/S1063776115040081

[18] M.I. Kopp, A.V. Tur, and V.V. Yanovsky, "Nonlinear Dynamo," arXiv:1612.08860v1 [astro-ph.EP] (2016). https://arxiv.org/abs/1612.08860v1

[19] P.N. Brandt, G.B. Scharmer, S. Ferguson, R.A. Shine, T.D. Tarbell, and A.M. Title, "Vortex flow in the solar photosphere," Nature, **335**, 238–240 (1988). https://doi.org/10.1038/335238a0

[20] M.I. Kopp, and V.V. Yanovsky, "Generation of large-scale magnetic-vortex structures in stratified magnetized plasma by a small-scale force," Phys. Plasmas, **31**, 082301 (2024). https://doi.org/10.1063/5.0214000

[21] S.I. Braginskii, "Transport processes in plasma," in: *Reviews of Plasma Physics*, Vol. 1, edited by M.A. Leontovich, (Consultants Bureau, New York, 1965), pp. 205-311.

[22] G.Z. Gershuni, and E.M. Zhukhovitskii, *Convective Stability of Incompressible Fluids*, (Keter Publishing House, Jerusalem, 1976).

ВИНИКНЕННЯ ВЕЛИКОМАСШТАБНИХ МАГНІТО-ВИХРОВИХ СТРУКТУР ДРІБНОМАСШТАБНОЮ СПІРАЛЬНІСТЮ В СТРАТИФІКОВАНІЙ ЗАМАГНІЧЕНІЙ ПЛАЗМІ

М.Й. Копп[1], **В.В. Яновський**[1,2]

[1]*Інститут монокристаллов, Національна Академія Наук України, пр. Науки 60, 61072, Харків, Україна*

[2]*Харківський національний університет ім. В.Н. Каразіна, майдан Свободи, 4, 61022, Харків, Україна*

В роботі виявлено новий тип нестійкості, що призводить до генерації вихрових рухів та магнітних полів у плазмовому шарі з постійним градієнтом температури під дією однорідної сили тяжіння та вертикального магнітного поля. Аналіз проводиться у межах електронної магнитогидродинамики (ЕМГД) з урахуванням термомагнітних ефектів. Отримано нову великомасштабну нестійкість типу α-ефекту, що сприяє генерації великомасштабних вихрових і магнітних полів. Ця нестійкість виникає внаслідок спільної дії зовнішнього однорідного магнітного поля, орієнтованого перпендикулярно до плазмового шару, і маломасштабної спіральної сили. Зовнішня сила моделюється як джерело дрібномасштабних коливань у полі швидкості електронів, що характеризується малим числом Рейнольдса ($R \ll 1$). Наявність малого параметра у системі дозволяє застосувати метод багатомасштабних асимптотичних розкладів. У третьому порядку за кількістю Рейнольдса отримано систему нелінійних рівнянь, що описують еволюцію великомасштабних вихрових та магнітних збурень. Обговорюється також новий ефект, пов'язаний із впливом термосили (ефект Нернста) на великомасштабну нестійкість. Показано, що збільшення параметра Нернста зменшує коефіцієнт α і тим самим пригнічує розвиток великомасштабної нестійкості. За допомогою чисельного аналізу отримано стаціонарні рішення рівнянь вихрового та магнітного динамо у вигляді локалізованих структур спірального типу.

Ключові слова: *електронна магнітогідродинаміка; багатомасштабні асимптотичні розкладання; дрібномасштабна сила; α-ефект; локалізовані структури*